ISSN 1063-7796, Physics of Particles and Nuclei, 2015, Vol. 46, No. 3, pp. 452–474. © Pleiades Publishing, Ltd., 2015.
Original Russian Text © Yu.G. Asadov, Yu.I. Aliyev, A.G. Babaev, 2015, published in Fizika Elementarnykh Chastits i Atomnogo Yadra, 2015, Vol. 46, No. 3.

Polymorphic Transformations in Cu_2Se, Ag_2Se, AgCuSe and the Role of Partial Cation–Cation and Anion–Anion Replacement in Stabilizing Their Modifications

Yu. G. Asadov, Yu. I. Aliyev, and A. G. Babaev

Abdullaev Institute of Physics, Azerbaijan National Academy of Sciences, Baku, AZ-1143 Azerbaijan
e-mail: yusifasadov@rambler.ru

Abstract—A review of studies of the crystalline structure of copper and silver chalcogenides is given. These materials have diverse physical properties making them promising in practical applications. Physical properties of crystals are determined by chemical composition, crystalline structure, and the influence of external conditions. In this work we carried out the analysis of published results on the crystalline structures of copper and silver chalcogenides at high and low temperatures. The inconsistency of published data on the crystal lattice parameters is noted. We also present our own results on the temperature dependence and the features of phase transitions in copper and silver chalcogenides with different composition.

DOI: 10.1134/S106377961503003X

1. INTRODUCTION

In modern solid state physics, crystallography, and mineralogy, the behavior of substances under the conditions determined by a large number of external parameters such as temperature, pressure, electric and magnetic fields, etc., is studied. Various processes occur in crystals depending on the external conditions, such as polymorphic transitions, recrystallization, disassembling of solid solutions, thermal destruction, ordering and disordering, etc., which drastically alter the physical and mechanical properties of solids with a constant chemical composition.

Polymorphism is among the most important problems in solid state physics, when one crystal structure is destroyed, and a nucleus of the crystal having an absolutely new crystalline structure is formed in the locality of this destruction. The greatest scientific and practical interest is the study of polymorphic transformations in crystals having stoichiometric and nonstoichiometric composition. The mechanism of phase transformations, as well as the existence of high-temperature crystalline modifications in modern crystallography, is investigated using the methods of high-temperature X-ray diffraction. In addition, obtaining the X-ray patterns at different temperatures allows one to determine the lattice parameters and to study thermal expansion along different crystallographic directions. When studying mechanism of polymorphic transformations along with structural data, it is useful also to have thermodynamic data of crystalline modifications. To study the mechanism of polymorphic transformations in optically opaque crystals, the use of copper and silver chalcogenides, which are rich in polymorphic transformations, is more convenient. Due to this, these systems have been chosen in this paper as the objects of investigation.

To determine the nature of polymorphic transformations, it is necessary to perform accurate measurements of lattice parameters, atomic volume, and density, as well as the thermal expansion coefficients of the present modifications as a function of the temperature. Exact determination of these parameters has always been an urgent problem in solid state physics because all physical properties of crystals are determined, first of all, by the features of their crystalline structure. Appropriate studies allow one to obtain extensive experimental data for determining atomic mechanism of polymorphic transformations and crystal lattice dynamics.

The binary and ternary compounds and non-stoichiometric compositions of the copper and silver chalcogenides are strongly affected by a large number of intrinsic lattice defects. The high interest in this class of materials is caused by various optical and electrical properties, making them useful for manufacturing thermoelectric transducers, photoresistors, photodiodes etc.

Practical application of their important physical properties requires a detailed study of real structure, structural phase transformations, establishment of the mechanism of transformations, and the regions of stability for each of modifications, etc.

In this review we consider polymorphous transformations in Cu_2Se, $Cu_{1.80}Zn_{0.20}Se$, $Cu_{1.75}Zn_{0.05}Se$, Ag_2Se, AgCuSe, $Ag_{1\pm x}Cu_{1\mp x}Se$, $AgCuSe_{1-x}(S,Te)_x$.

Table 1. Elementary cell parameters for a low-temperature Cu_2Se crystalline modification

Lattice type	Lattice parameters			Transition temperature, K	Year of study	Authors
	a (Å)	b (Å)	c (Å)			
Tetragonal	11.49	–	11.72	376	1945	W. Borchert [6]
Tetragonal	11.63	–	11.40	–	1959	P. Gunod [7]
Orthorhombic	8.17	6.68	10.5	393	1969	M. Kazinets [9]
Cubic	5.813	–	–	–	1957	B. Kotovich, F. Kimenetsky [10]
Orthorhombic	4.118	7.032	20.38	403	1971	A. N. Stevels, F. Jeellinek [11]
Not determined lattice type	–	–	–	–	1890	M. Vellati, S. Lussaa [12]
Not determined lattice type	–	–	–	no transition before 573	1969	S. K. Sharma [13]
Not determined lattice type	–	–	–	404	1966	Heyding [14]
Not determined lattice type	–	–	–	404	1970	B. Keni, S. Michel [15]

2. CRYSTALLINE STRUCTURE OF Cu_2Se

On the phase diagram, the Cu_2Se compound exists in the range of 38.38 at % Se [1, 2]. Its density and melting point are $\rho = 6.749$ g/cm^3 and $T = 1386$ K [3].

There are known two modifications of Cu_2Se. The structure of a low-temperature α-phase in Cu_2Se was not studied. The structure of a high-temperature cubic phase was first determined in [4]. At 443 K, the elementary cell parameter is $a = 5.840$ Å and a spatial symmetry group is $F\bar{4}3m$. A part of Cu atoms and all Se atoms occupy the positions of Zn and S atoms in zinc blend (4Se-4d), 000, 4Cu-4(c) 1/4 1/4 1/4. The remaining atoms are statistically arranged in positions 4(b)1/2 1/2 1/2 and 16(e) xxx at $x = 2/3$. The selectivity is not observed when filling the voids with copper atoms. According to [5, 6], position 16(e) with $x = 2/3$ is occupied with a significantly smaller probability. The distribution of Cu^{1+} atoms depends on the composition and temperature. Since the copper atoms are very mobile, this leads to high diffusion velocity.

The existence of homogeneous phases in the $Cu_{2-x}Se$ composition with deficit of Cu^{1+} is also closely related to the mobility of Cu ions. The cubic modification is also stable at room temperature upon considerable deficit of copper atoms. It also exists in nature in mineral form (berzelite) [7–17]. At normal temperature, the elementary cell parameter of $Cu_{2-x}Se$ ($x = 0.5$) is $a = 5.72$ Å.

There are ambiguities in the literature relative to the crystalline structure of a low-temperature α-Cu_2Se phase and the temperature of polymorphic transformation. These data are given in Table 1.

In [7], it is asserted that there is an equilibrium region of an ordered phase for Cu_2Se in the limits from room temperature to 393 K. The corresponding ordered phase with a tetragonal lattice has elementary cell periods $a = 11.49$ Å, $c = 11.72$ Å, while at temperatures greater than 393 K the disordered phase has the fcc structure with an elementary cell parameter $a =$ 5.82 Å. The author of this work erroneously assumes that this phase transformation in Cu_2Se has a martensitic nature and he claims that the "transformation occurs simultaneously over the whole sample without formation of nucleation centers". This, in the author's opinion, is due to high transition rate and the lack of temperature dependence.

3. CRYSTALLINE STRUCTURE OF THE α- AND β-Ag_2Se MODIFICATIONS

According to [1, 2], silver and selenium may form a single compound, namely Ag_2Se containing 26.79 at % of Se.

The literature data on crystalline structure of a low-temperature modification of α-Ag_2Se are contradictory [18, 19]. In [20], only a single table of the interplanar distances is presented, calculated from the low-temperature X-ray powder pattern of α-Ag_2Se. In [21], the electron diffraction studies of Ag_2Se films obtained in vacuum shows that the low-temperature modification is crystallized in the tetragonal syngony with lattice parameters $a = 7.08$ Å and $c = 4.98$ Å. These authors also report that upon the reverse transformation from a high-temperature to a low-temperature modification, the transformation proceeds through intermediate bcc tetragonal lattice modification with lattice parameters $a = 4.98$ Å, and $c = 4.78$ Å. In [22, 23], the Ag_2Se films were obtained at the surface of KCl and NaCl crystals by vacuum evaporation of Se and Ag. It was shown that metastable fcc modification with lattice parameter $a = 5.65$ Å is obtained at room temperature from the film obtained at 573 K, while the rhombic modification with lattice parameters $a = 7.06$ Å, $b = 7.76$ Å, $c = 4.34$ Å is obtained from the fcc modification at 473 K.

According to [6], the low-temperature Ag_2Se modification has a pseudocubic structure with lattice parameter $a = 4.978$ Å. The author of this work assumes both that Ag_2Se modifications are characterized by the same arrangement of Se atoms and that transition to a high-temperature modification is caused

Table 2. Scheme of structural transformations in Ag_2Se [26]

Cubic $a = 7.046$ Å [24]		
$[001]_t \| [110]_k$ $[100]_t \| [110]_k$	~406 K	$[100]_m \| [110]_k$ $[010]_m \| [110]_k$
Monoclinic $a = 6.91$ Å, $b = 7.87$ Å, $c = 4.23$ Å, $\beta = 99.58°$ [25]		
406 K	$[100]_{R.T.} \| [100]_m$ $[010]_{R.T.} \| [010]_m$	~318 K
Tetragonal [19]	Orthorhombic [23]	Triclinic [25]
$a = 7.08$ Å $c = 4.98$ Å	$a = 7.06$ Å $b = 7.80$ Å $c = 4.34$ Å	$a = 7.0$ Å, $\alpha = 92°$ $b = 7.8$ Å, $\beta = 91.5°$ $c = 4.3$ Å, $\gamma = 92°$

Table 3. Atomic positions in α-Ag_2Se

Atom	Coordinates		
	x	y	z
Ag(I)	0.121	0.225	0.022
Ag(II)	0.393	0	0
Ag(III)	0.378	0.500	0
Se	0.298	0.275	0.522

Table 4. Interatomic distances in α-Ag_2Se (in Å)

Atom	Ag(I)	Ag(II)	Ag(III)	Se
Ag(I)	2.62, 2.91	2.61	2.82	2.54, 2.98
Ag(II)	–	2.64	3.925	3.06, 3.19
Ag(III)	–	–	2.77	2.89, 2.93
Se	–	–	–	3.53, 3.76

Table 5. Atomic coordinates in α-Ag_2Se (in Å)

Atom	Coordinates		
	x	y	z
Ag(I)	0.375	0.619	0.456
Ag(II)	0.978	0.279	0.361
Se	0.608	0.485	0.149

Table 6. Interatomic distances in α-Ag_2Se (in Å)

Atom	Se	Se	Se	Se
Ag(I)	2.62	2.71	2.79	2.86
Ag(II)	2.62	2.74	2.81	–

by the disordering of Ag atoms. In addition, the author cites a third rhombic modification that is transformed into a pseudocubic modification after some time. The elementary cell parameters of this rhombic modification are $a = 7.046$ Å, $b = 14.32$ Å and $c = 7.82$ Å.

In [24], two different low-temperature modifications were found as a result of several heating/cooling cycles in some areas of the Ag_2Se film. The first lattice has the triclinic structure with lattice parameters $a = 7.0$ Å, $b = 7.6$ Å, $c = 4.3$ Å, $\alpha = 92°$, $\beta = 91.5°$, $\gamma = 92°$, the second has a monoclinic structure. In [25], the authors also studied the state of Ag_2Se in the form of a thin film. It was shown that at low temperatures in the film coexist simultaneously tetragonal, rhombic, and triclinic Ag_2Se modifications. Table 2 shows a scheme of structural transformations given in this work.

From the foregoing it is clear that different researchers give different values for the lattice parameters and different syngonies for a low-temperature Ag_2Se crystalline modifications: cubic [22], tetragonal [21–27], rhombic [23, 28–38], monoclinic [24–40] and triclinic [25, 27, 39]. It is worth noting that the conditions of sample manufacturing and the methods of studying were different. This is especially true in the study of thin-film states.

For this reason, different types of structures were associated with a single low-temperature Ag_2Se modification. The main reason in ambiguous results of different authors obtained for thin-film samples is probably due to the formation of various stoichiometric phases, whose composition was not controlled.

In most works [26, 31, 41] where massive samples were studied, the temperature of polymorphic $\alpha \longrightarrow \beta$ transition in Ag_2Se lies in the interval of 406–413 K. In [42], however, the $\alpha \longrightarrow \beta$ transitions in Ag_2Se were observed at 433 K, and the authors concluded that a higher transition temperature is characteristic for thin-film samples.

Crystalline structure of the low-temperature modification was considered in detail [31, 36]. In [31], rhombic structure was determined by electron diffraction and the lattice parameters are equal to $a = 7.05$ Å, $b = 7.85$ Å, and $c = 4.33$ Å. The elementary cell consists of $Z = 4Ag_2Se$ with spatial group $P222_1$. Tables 3 and 4 give the interatomic distances in Ag_2Se.

In [36], rhombic α-Ag_2Se modification was also proposed with lattice parameters $a = 4.333$ Å, $b = 7.062$ Å, $c = 7.764$ Å, $Z = 4$, and spatial group D_2^4–$P2_12_12_1$. The atomic positions and interatomic distances in α-Ag_2Se are listed in Tables 5 and 6.

In rhombic lattice, Ag(I) and Ag(II) ions occupy tetrahedral and triangular sites, surrounded by selenium atoms. In both works, the syngonies, elementary cell parameters, and atomic numbers are the same, whereas the spatial symmetry groups are different: in [31], spatial symmetry group is D_2^2–$P222_1$, while in

[33] it is $D_2^4-P2_12_12_1$. In the case of $P222_1$ spatial group, the forbidden reflexes correspond to the (00l) planes at $l = 2n$. In the case of $P2_12_12_1$ spatial group, the reflexes (hkl) are admissible, whereas the (h00), (0k0), and (00l) reflexes are forbidden at $h = k = l = 2n$.

In what follows, we use the $P222_1$ spatial group in processing experimental data. The choice of this structural model is not related with falseness of the $P2_12_12_1$ group.

Despite the fact that a low-temperature Ag_2Se modification is crystallized in rhombic structure, it is very similar to the Ag_2S monoclinic structure. Figure 1 shows atomic arrangement in both structures in the (011) projection. Structural study of a high-temperature β-Ag_2Se modification [26] confirmed its similarity to the β-Ag_2S structure: Se^{2-} ions form the bcc structure, while the Ag^{1+} ions are located in a large number of voids of this lattice, preferably in the largest of them. In β-Ag_2S, the lattice parameter slightly increases with respect to β-Ag_2Se: $\Delta a = (4.98 - 4.88)$ Å = 0.1 Å. This difference is equal to the difference in ionic radii of Se and S ions.

According to [26], the lattice parameter in β-Ag_2Se is $a = 4.983$ Å, $Z = 2Ag_2Se$, and the spatial group is O_h^5-Fm3m. Figure 2 shows an idealized bcc cubic elementary cell.

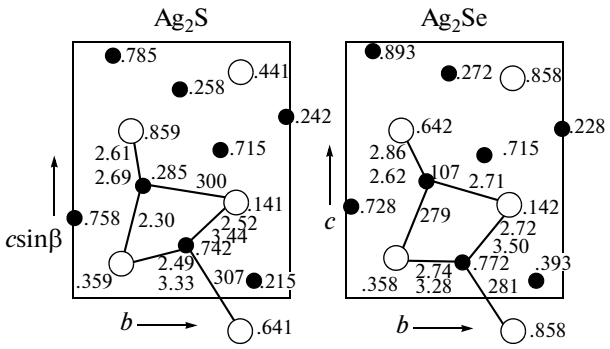

Fig. 1. Projections of the α-Ag_2S monoclinic structure and orthorhombic α-Ag_2Se structure in the [011] direction.

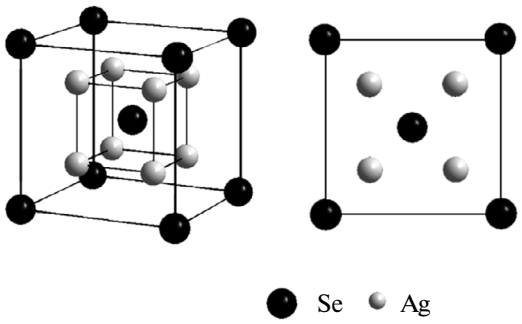

Fig. 2. An ideal cubic bcc elementary cell of β-Ag_2S(Se).

4. CRYSTALLINE STRUCTURE OF AgCuSe

The AgCuSe compound is formed at a temperature of 1033 K in peritectic reaction and has the composition ratio $Ag_2Se : Cu_2Se = 1 : 1$ [43, 44]. Polymorphic transformations in Ag_2Se and Cu_2Se compounds left the trace in their ternary alloys. At temperatures below 473 K the Ag_2Se-based and Cu_2Se-based solid solutions undergo eutectoid decompositions [42–46].

In [47], using a natural mineral sample, it was shown for the first time that AgCuSe is crystallized at room temperature into a tetragonal structure with lattice parameters $a = 4.075$ Å, $c = 6.29$ Å, spatial group P4/nmm, $Z = 2$AgCuSe. The calculated density $\rho = 7.91$ g/cm^3 corresponds to the experimentally measured density $\rho = 7.67$ g/cm^3.

In [48], the samples of one and the same mineral were used in structural studies.

The AgCuSe is contained in dendritic inclusions of calcite. The samples underwent etching in the HCl acid and milling in an iron grinder at a temperature of liquid nitrogen. Processing was carried out at a low temperature to exclude plastic deformations of samples. For diffraction studies, single crystals with a size of about 0.1 mm were chosen. At a first approximation, spatial symmetry group and the lattice parameter obtained in [48] were confirmed. However, the analysis of Weissenberg's pictures obtained from several crystals showed that the crystal has a rhombic symmetry if we take into account additional weak reflexes which appeared on them. This means that the size of an elementary cell corresponding to the b axis direction [48] increases by five times, i. e. $a = 4.105$ Å, $b = 4.07 \times 5 = 20.35$ Å, $c = 6.31$ Å. Figure 3 shows an idealized AgCuSe structure.

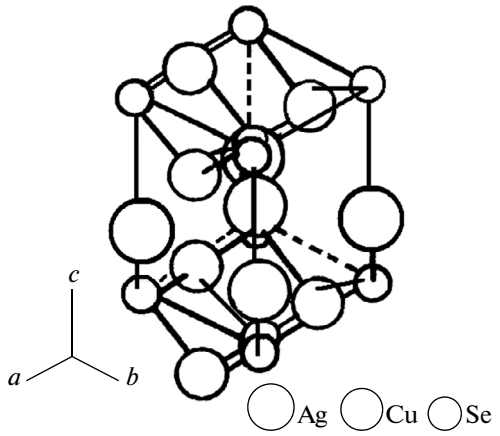

Fig. 3. Crystalline structure of AgCuSe.

Silver atoms in this structure are located in the planes perpendicular to the c axis. Each Ag atom is surrounded by four other Ag atoms at distances of 2.96 Å; a Se atom is located at a closer distance

Table 7. The atomic composition in the above structures

Composition	Cu, at %	Ag, at %	Zn, at %	S, at %	Se, at %	Te, at %
Cu_2Se	61.677	–	–	–	38.323	–
Ag_2Se	–	66.6666	–	–	33.3333	–
AgCuSe	33.3333	33.3333	–	–	33.3333	–
$Ag_{1.5}Cu_{0.5}Se$	16.6666	49.9999	–	–	33.3333	–
$Ag_{0.4}Cu_{1.6}Se$	45.4311	19.2836	–	–	35.2853	–
$Cu_{1.80}Zn_{0.20}Se$	55.458	–	6.162	–	38.380	–
$Cu_{1.75}Zn_{0.05}Se$	57.488	–	1.690	–	40.822	–
$AgCuSe_{0.5}S_{0.5}$	27.9995	47.5383	–	7.0651	17.3972	–
$AgCuSe_{0.5}Te_{0.5}$	33.3333	33.3333	–	–	16.6666	16.6666

of 2.67 Å, four other atoms are located at distances of 3.59 Å and one atom at a distance of 3.64 Å. Therefore, Se atoms form layers of flattened tetrahedrons, in which each angle is divided by similar tetrahedrons. Each Se atom has four neighboring Se atoms at distances of 3.30 Å. Cu atoms are located inside a flattened tetrahedron. They are not located at the center of the tetrahedron, but closer to one of the long ribs, lying at a distance of 2.06 Å from one pair of selenium atoms and at a distance of 2.50 Å from another pair. The closest Cu–Ag spacing is 2.98 Å. It was noted that one of the Cu–Se distances is greater than one could expect, while the other interatomic distances seem to be reasonable. One of the features of AgCuSe structure is the fact that each Ag atom is closely bound to a Se atom and binding forces in this structure may partly depend on the metallic Ag–Ag bonds.

As was also noted in this work, orthorhombic low-temperature modification of AgCuSe is converted into a cubic one at temperatures of 463–468 K and this transformation is reversible.

From the above it follows that in AgCuSe ternary compounds with two types of cations, unlike Ag_2Se and Cu_2Se binary compounds, the problem of polymorphism remains incomplete to date.

5. SYNTHESIS AND PHYSICAL-CHEMICAL ANALYSIS OF Cu_2Se, Ag_2Se, AgCuSe, $Ag_{1.5}Cu_{0.5}Se$, $Ag_{0.4}Cu_{1.6}Se$, $Cu_{1.80}Zn_{0.20}Se$, $Cu_{1.75}Zn_{0.05}Se$, $AgCuSe_{0.5}S_{0.5}$, $AgCuSe_{0.5}Te_{0.5}$

To obtain homogeneous samples of these compositions we used a method of direct synthesis, i. e. chemical interaction of initial reagents. For synthesized compositions, quartz ampoules of high-quality with an inner diameter of 1 cm and a length of 10 cm were used as the reactor. The ampoules were filled with initial components, namely Cu, Ag, Zn, S, Se, and Te in the amount needed for each composition. Then they were pumped out to a pressure of 10^{-3} MPa, and sealed. The components used in the synthesis are electrolytic copper; Ag and Zn with purity of 99.999; and Se, S and Te of brand B5. The amounts of components used in the synthesis for each composition are given in Table 7.

The same conditions were chosen in synthesis of these compounds. To prevent the explosion of ampoules, as well as to reach complete diffusion of melted S, Se and Te with Cu, Ag, Zn, we slowly increased the temperature in the oven up to the melting point of Se ($T = 493$) in one case, and up to the melting points of S ($T = 393$ K) and Ne ($T = 725$ K) in other cases, and each composition was kept at the corresponding temperature for four hours. After that, we increased the temperature in the oven at a rate of 50 K/h above the melting point of AgCuSe ($T =$ 1039 K). Having been kept at this temperature for five hours with cyclic vibration, the ampoules with samples were slowly cooled to 400 K and annealed at this temperature during 200 h for better homogenization. To establish the individuality of each composition, microstructural and X-ray analysis were carried out.

5.1. Microstructural Analyses of Cu_2Se, Ag_2Se, and AgCuSe

For microstructural studies, flat samples were cut from synthesized compositions. First of all, the samples of all compositions were polished. Accurate preparation of microsections is extremely important, since it determines correctness of the microstructure interpretation. If microsections were prepared badly, the erroneous interpretation of microstructures is nearly always inevitable. The main point in preparing microsections is preventing the damage of the surface of microsections due to the changes in microstructure of the surface layer of material caused by deformation or heating. Grinding and polishing should be carried out so that the surface layer had minimal distortions and deformations. This is necessary in determining real the microstructure of material after etching. In addition, the pits and scratches should not be observed on the surface of the polished section. The preparation of sample microsections includes the following main procedures: (a) sample cutting; (b) polishing; (c) etching.

Table 8. Measurement results of the lattice parameters using powder roentgenograms and compositions of each synthesized sample

Structures and compositions	Lattice parameters			β	Z	Spatial group	V, Å^3	ρ, g/cm^3
	a, Å	b, Å	c, Å					
Cu_2Se—orthorhombic	4.1168	7.0320	20.3472	–	12	–	589.038	6.968
$Cu_{1.80}Se$— fcc	5.7356	–	–	–	4	Fm3m	188.685	6.804
$Cu_{1.80}Zn_{0.20}Se$—orthorhombic	4.1274	7.0327	20.3618	–	12	–	591.011	6.957
$Cu_{1.80}Zn_{0.20}Se$—fcc	5.7560	–	–	–	4	Fm3m	190.705	7.187
$Cu_{1.75}Zn_{0.05}Se$—fcc	5.741	–	–	–	4	Fm3m	189.218	6.787
Ag_2Se—orthorhombic	7.065	7.847	4.325	–	4	$P222_1$	239.779	8.164
AgCuSe—orthorhombic	4.104	20.350	6.310	–	10	P4/nmm	526.988	7.888
$Ag_{0.4}Cu_{1.6}Se$–AgCuSe	4.104	20.350	6.310	–	10	P4/nmm	526.988	7.885
$Ag_{0.4}Cu_{1.6}Se$–Ag_2Se	4.333	7.062	7.762	–	4	$P222_1$	237.576	8.237
$Ag_{1.5}Cu_{0.5}Se$–Ag_2Se	4.333	7.062	7.764	–	4	$P222_1$	237.576	8.237
$Ag_{1.5}Cu_{0.5}Se$–AgCuSe	4.105	20.350	6.310	–	10	P4/nmm	527.117	7.885
$AgCuSe_{0.5}S_{0.5}$–$Cu_{1.96}S$	26.827	15.745	13.565	90.13°	8	$P2_1/n$	5729.735	5.807
$AgCuSe_{0.5}S_{0.5}$–AgCuSe	4.086	20.524	6.279	–	10	P4/nmm	526.564	7.154
$AgCuSe_{0.5}Te_{0.5}$–Cu_2Te	7.319	22.236	36.458	–	104	P6mmm	5933.368	7.407
$AgCuSe_{0.5}Te_{0.5}$–AgCuSe	4.107	20.421	6.299	–	10	P4/nmm	528.058	7.883
$AgCuSe_{0.5}Te_{0.5}$—cube	7.715	–	–	–	8	Fd3m	459.206	7.940

Polishing is the final stage in the process of mirror-smooth surface fabrication being freed of scratches. The obtaining of such surface is necessary for performing correct analysis.

To determine the structure of synthesized materials, the samples in the form of plates were cut from each ingot. Their surfaces were ground and then polished using a diamond paste. To study the characteristics of material, the polished surface layer was removed by etching in solutions composed of 50 % HNO_3 + 50% H_2O and 1 : 1 HNO_3, 1 : 1 HCl. Micrographs of the surfaces of each sample were obtained using a MIM-7 metallographic microscope in reflection mode.

As one can see from micrographs of surfaces in Fig. 5, the obtained single-phase compositions have the large-block structures without any inclusions.

The structure, size, and arrangement of blocks on each sample are different. Because of the closeness of chemical composition, the corresponding two-phase samples were indistinguishable on photomicrographs. The X-ray analysis is completely indispensable when revealing the presence of different phases in materials with the same compositions.

5.2 X-ray Analysis

For determining single-phase structures with the same composition, X-ray analysis is indispensable. Each phase has a unique X-ray pattern, i. e. the diffraction reflexes and their intensities when different phases are present in synthesized substance.

For determining the phase ratios of compositions, powder samples were fabricated from each synthesized ingot. The powders of each composition were loaded in glass capillaries with an inner diameter of ~0.8 mm. The pressed samples were prepared by extrusion from one end of the capillary by using a wire of ~0.7 mm in diameter which produced the samples in the form of wire. The X-ray pictures for each composition were obtained in a RKD-57.3 chamber after 16 hour exposition using the CuK_α radiation line with λ =1.5418 Å and Ni filter. Table 8 shows the calculation results of lattice parameters. As one can see from these results obtained at room temperature, Cu_2Se, $Cu_{1.80}Se$, $Cu_{1.75}Zn_{0.05}Se$, Ag_2Se and AgCuSe samples are single-phase, $Cu_{1.80}Zn_{0.2}Se$, $Ag_{0.4}Cu_{1.6}Se$, $Ag_{1.5}Cu_{0.5}Se$ and $AgCuSe_{0.5}S_{0.5}$ are two-phase, and $AgCuSe_{0.5}Te_{0.5}$ are ternary.

As will be shown, at a high temperature all compositions are transformed into a cubic modification.

6. SINGLE CRYSTAL GROWING

The obtaining of single crystals with a low-temperature modification of chemical composition, which undergo one or more structural transformations from room temperature up to the melting point, is related with certain difficulties. The point is that the crystals of high-temperature modification always grow from melts and gaseous phase, whereas the crystals of low-temperature modification are obtained as a result of

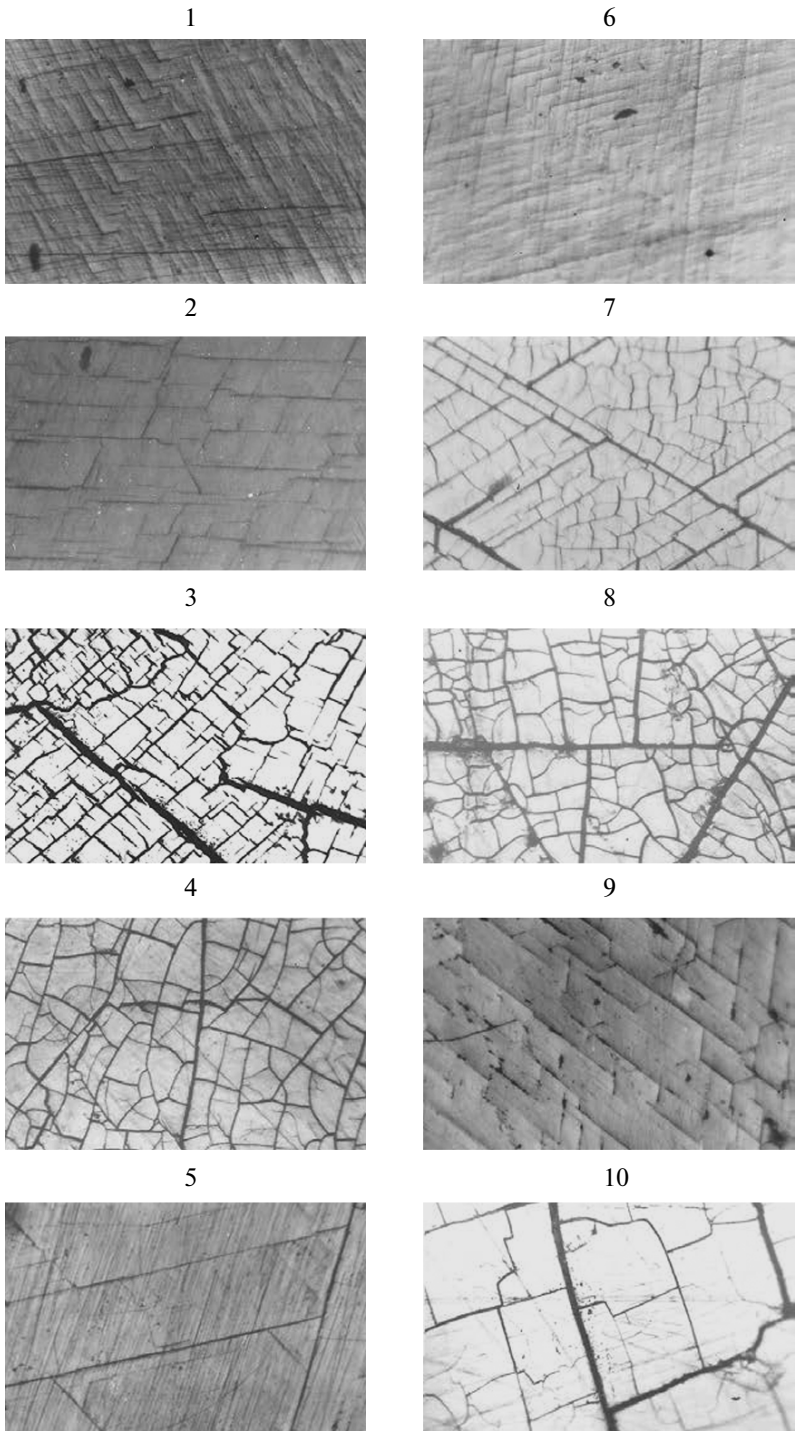

Fig. 4. Microstructures of Cu_2Se (1), $Cu_{1.80}Se$ (2), $Cu_{1.80}Zn_{0.20}Se$ (3), $Cu_{1.75}Zn_{0.05}Se$ (4), Ag_2Se (5), AgCuSe (6), $Ag_{0.4}Cu_{1.6}Se$ (7), $Ag_{1.5}Cu_{0.5}Se$ (8), $AgCuSe_{0.5}S_{0.5}$ (9) $AgCuSe_{0.5}Te_{0.5}$ (10) at a magnification factor of ×360.

structural transformations when cooling to room temperature.

It is worth noting that very often structural transformations are accompanied by considerable change in the volume, which leads to the appearance of stresses and to development of the substructure in crystals. Monocrystallinity of the low-temperature modification growing inside a high-temperature one depends mainly on the density difference. The modifications of polymorphic substances can be divided in three groups according to the difference in their densities.

(i) The density ρ_p of growing phase is lower than the density ρ_m of the matrix: $\rho_p < \rho_m$;

(ii) The density of growing phase is higher than the density of the matrix: $\rho_p > \rho_m$;

(iii) The densities of growing crystal and matrix are equal or slightly differ: $\rho_p = \rho_m$, $\rho_p \geq \rho_m$ or $\rho_p \leq \rho_m$.

In cases where $\rho_p < \rho_m$, the matrix is deformed in the process of transformation and very often cracks are formed. Each crack becomes the source of formation for many crystallization centers. As a result, single crystal is transformed into a polycrystal.

In case $\rho_p > \rho_m$ the contact between a growing crystal and the matrix becomes weaker and interfacial distance exceeds the interatomic distance. In this case, the growth of crystal in a new phase is terminated. The process of transformation is continued owing to formation of more and more new nucleation centers. In this case, a single crystal is transformed into a polycrystal, and it is impossible to obtain a single crystal from polycrystal.

In case $\rho_p \geq \rho_m$, $\rho_p \leq \rho_m$, and $\rho_p = \rho_m$, two types of transformation are usually observed: "single crystal $\rightleftharpoons$ single crystal" and "single crystal $\rightleftharpoons$ polycrystal". The second of these transformations occurs with the formation of plurality of nucleation centers and due to the imperfection of a matrix crystal. A single crystal with needed modification can be obtained from such a polycrystal at a certain number of transformations.

It was experimentally found that for growing single crystals of synthesized samples the most appropriate method is the combination of slow cooling and Bridgman's methods, which are used for growing crystals from melt.

After having been studied by X-ray phase analysis, the synthesized samples of $Ag_2S(Se,Te)$, AgCuS, $Ag_{2-x}Cu_xS$, $AgCuS_{0.5}(Se,Te)_{0.5}$ were placed in the ampoules manufactured of high-quality quartz tubes with a length of 10 cm and an inner diameter of 0.5 cm. The ampoules evacuated up to a pressure of 10^{-5} Pa, having the corresponding composition, were placed inside a vertical oven with three temperature zones. In the upper zone of the oven the temperature is 50 K higher than the melting point of a composition, while in the second it is 50 K lower. When the temperature of the sharp end of ampoule passes the melting point, the seed crystals of high-temperature modification are formed in the zone with lower temperature. The displacement of ampoule with a rate of 0.2 cm/h proved to be suitable for the growth of the nucleus of a high-temperature phase. With further displacement of the ampoule with crystals of high-temperature phase to the temperature range corresponding to the structural transformation, a single crystal of the fcc phase is transformed into a low-temperature phase. Then the ampoules in the third zone of the oven were annealed for three weeks below the temperature of structural transformation.

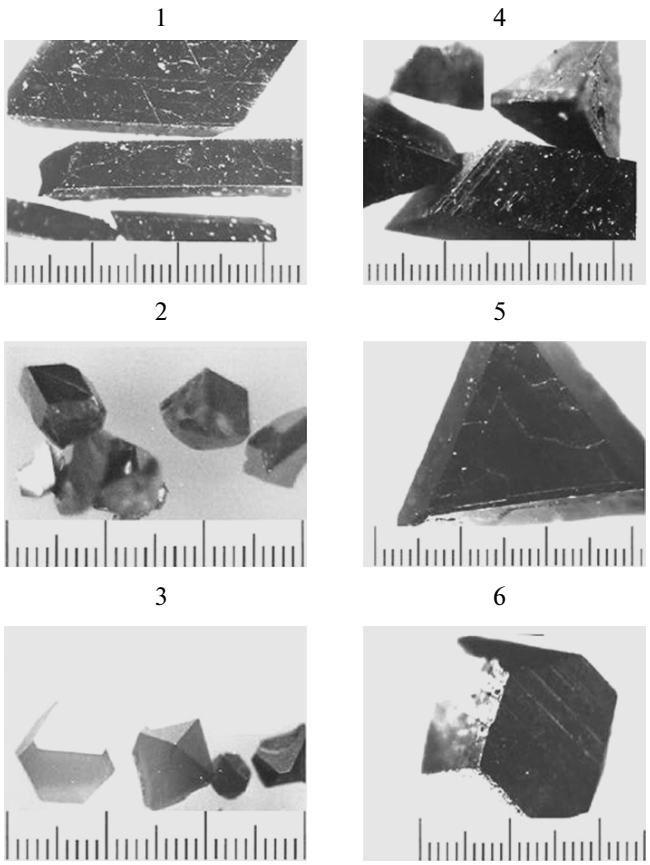

Fig. 5. Monocrystals of Cu_2Se (1), Ag_2Se (2), AgCuSe (3), $Cu_{1.80}Zn_{0.20}Se$ (4), $Ag_{1.5}Cu_{0.5}Se$ (5), $AgCuSe_{0.5}S_{0.5}$ (6).

Figure 5 shows single crystals obtained which became the objects of studying polymorphic transformations. The next section is devoted to the high-temperature study of polymorphic transformations and thermal expansion of separate modifications.

7. STRUCTURAL ASPECTS OF THE POLYMORPHIC TRANSFORMATIONS IN Cu_2Se

Single crystals of Cu_2Se easily cleaved in the [011] direction. For these crystals, seven distinct diffraction peaks were registered at room temperature in the interval of angles $10° < 2\theta < 90°$: (011), (022), (027), (040), (055), (0.0.18) and (400). All diffraction reflexes from the powder roentgenogram and single crystal are indexed in a low-temperature rhombic structure with elementary cell parameters $a = 4.118$ Å, $b = 7.032$ Å, $c = 20.360$ Å, $Z = 12$ [49–51].

After recording diffraction spectra at room temperature, crystal orientation was not changed, the oven was switched on and new experiments were carried out at temperatures of 323, 373, 405, 423, 473, 523 and 573 K. Before each registration of spectra, the temperature in the oven was kept constant during 30 min. The

Table 9. Thermal dependence of the Cu_2Se lattice period

T_{exp}, K	Modification	Lattice parameters			Z	Spatial group	V, Å^3	ρ, g/cm^3
		a, Å	b, Å	c, Å				
293	Orthorhombic	4.117	7.032	20.347	12	$P222_1$	589.061	6.968
323	Orthorhombic	4.118	7.034	20.351	12	$P222_1$	589.487	6.963
373	Orthorhombic	4.121	7.038	20.367	12	$P222_1$	590.716	6.948
405	Orthorhombic	4.125	7.042	20.380	12	$P222_1$	592.003	6.933
423	fcc	5.839			4	$F\bar{4}3m$	199.074	6.827
473	fcc	5.844			4	$F\bar{4}3m$	199.586	6.855
523	fcc	5.855			4	$F\bar{4}3m$	200.715	6.816
573	fcc	5.662			4	$F\bar{4}3m$	201.436	6.792

recording at 423 K already corresponded to a high-temperature fcc modification. In this case, all diffraction reflexes corresponding to a low-temperature rhombic modification disappear. Instead, new reflexes are registered in the same angular interval with indices (111), (222), (333) corresponding to a high-temperature fcc modification with elementary cell parameter $a = 5.836$ Å. It was established that the equilibrium temperature between modifications is $T_0 = 407 \pm 1$ K [52].

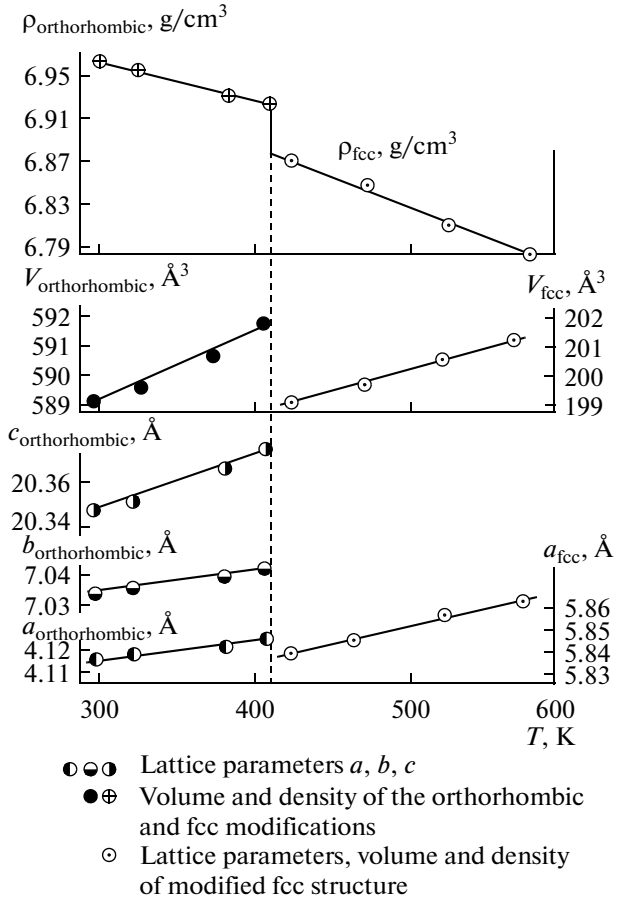

Fig. 6. Temperature dependence of the lattice parameters, volume, and density of the orthorhombic fcc Cu_2Se crystalline modifications.

Using diffraction spectra at 298, 323, 373, and 405 K, the lattice parameters of the rhombic structure were calculated, while the parameters for the fcc structure were calculated at 423, 473, 523, and 573 K. The calculation results are shown in Table 9 and Fig. 6.

The thermal expansion coefficients corresponding to the basic crystallographic directions were calculated by using lattice parameters of the rhombic and fcc modifications. These results are listed in Table 10. One can see that thermal expansion coefficients of the rhombic modification are positive and the corresponding surface has the form of ellipsoid, while for the fcc modification the surface of these coefficients has the spherical shape.

According to the calculated dependences of the densities of rhombic and fcc modifications, the density of these modifications at equilibrium ($T = 407$ K) changes abruptly by 0.062 g/cm^3 (Fig. 6). An insignificant density change of crystalline modifications allows one to obtain single crystals of low-temperature rhombic modification during triple structural transformation. The micrograph and the Laue picture in Fig. 7 confirm this conclusion.

It is worth noting that the concentration changes occur with increasing multiplicity of transformations (more than 10), i.e. the transition from Cu_2Se to $Cu_{2-x}Se$ ($x = 0.2$) takes place with copper precipitation at the boundaries of $Cu_{2-x}Se$ blocks. This nonstoichiometric composition has also the fcc lattice with $a = 5.740$ Å; it is stable in the interval between the room temperature and the melting point.

The lattice periods in the temperature interval of 299–573 K calculated from the changes in reflection

Table 10. Thermal expansion of the orthorhombic and fcc Cu_2Se crystalline modifications ($\times 10^6$ K^{-1})

T, K	$\alpha_{[100]}$	$\alpha_{[010]}$	$\alpha_{[001]}$	$\bar{\alpha} = \frac{\alpha_{[100]} + \alpha_{[010]} + \alpha_{[001]}}{3}$	$\beta = \alpha_{[100]} + \alpha_{[010]} + \alpha_{[001]}$
293–323	8.097	9.480	6.553	8.043	24.130
293–373	12.145	10.666	12.287	11.699	35.098
293–405	17.350	12.697	14.481	14.843	44.528
423–473	17.126			17.126	51.378
423–523	27.402			27.402	82.206
423–573	26.260			26.260	78.780

Table 11. Temperature dependence of the $Cu_{1.80}Se$ crystal lattice period

T_{exp}, K	Modification	Lattice parameters	Z	Spatial group	V, Å^3	ρ, g/cm^3
		a, Å				
299	fcc	5.734	4	Fm3m	188.527	6.772
383	fcc	5.747	4	Fm3m	189.527	6.733
473	fcc	5.767	4	Fm3m	191.801	6.663
573	fcc	5.773	4	Fm3m	192.394	6.642

angles corresponding to the (111), (222), and (333) peaks are given in Table 11.

Table 12 shows the values of thermal expansion coefficients in temperature interval of 299–573 K calculated from the lattice parameters. In this case, the surface of constant thermal expansion has a spherical shape.

8. STRUCTURAL ASPECTS OF THE POLYMORPHIC TRANSFORMATIONS IN $Cu_{1.80}Zn_{0.20}Se$

Single $Cu_{1.80}Zn_{0.20}Se$ and Cu_2Se crystals were easily cleaved along the (011) plane. The samples in the form of the plates with dimensions of $4 \times 4 \times 1$ mm suitable for X-ray study were cleaved from crystalline ingot.

Table 12. Thermal expansion of the fcc modification of $Cu_{1.80}Se$ crystal ($\times 10^6$ K^{-1})

T, K	$\alpha_{[100]}$	$\bar{\alpha} = \frac{3\alpha_{[100]}}{3}$	$\beta = 3\alpha_{[100]}$
299–383	26.99	26.99	80.97
299–473	33.08	33.08	99.24
299–573	24.82	24.82	74.76

Six diffraction reflexes were recorded for these samples within an angular interval of $10° \le 2\theta \le 70°$ at room temperature. These reflexes are similar to those observed on the roentgenogram of $Cu_{1.80}Zn_{0.20}Se$ powder, corresponding to the rhombic and high-tempera-

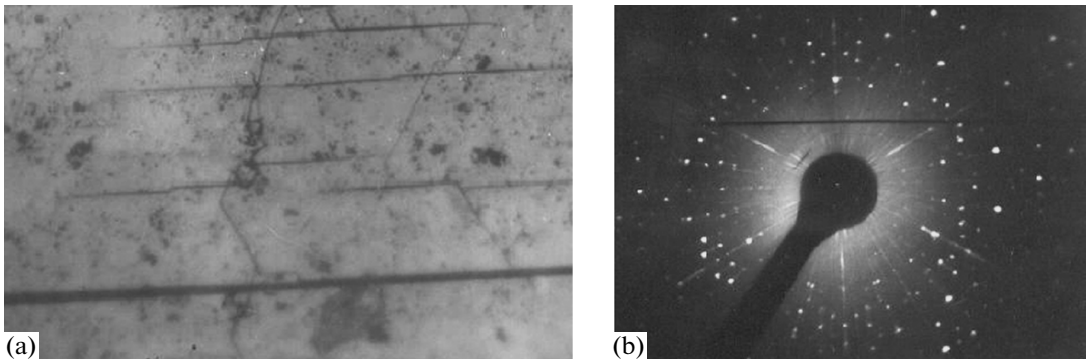

Fig. 7. Micrograph (a) and Laue pattern (b) of the Cu_2Se crystal after threefold transformation.

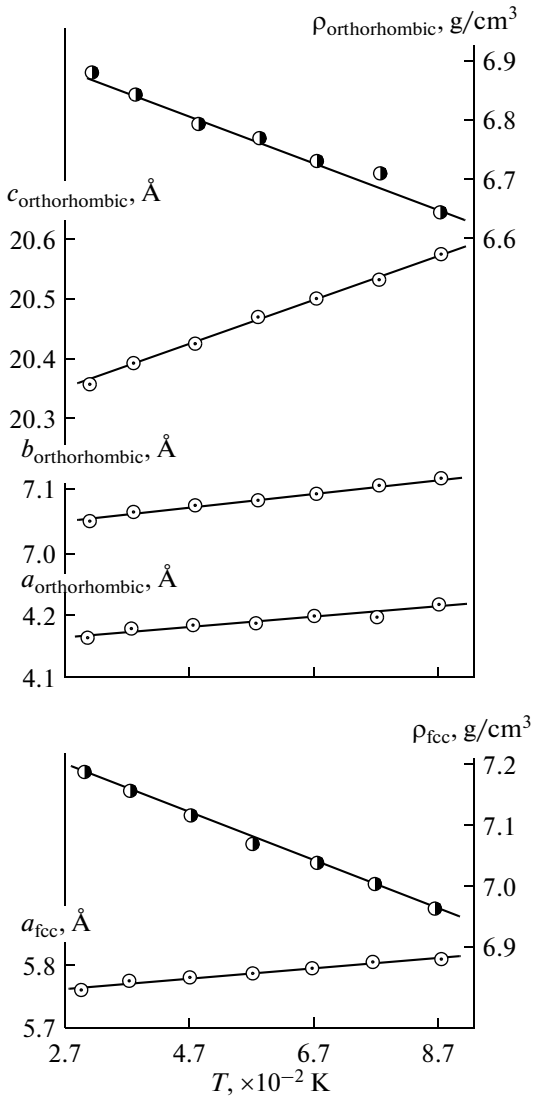

Fig. 8. Temperature dependence of the elementary cell parameters and densities of the orthorhombic and fcc $Cu_{1.80}Zn_{0.20}Se$ crystalline modifications.

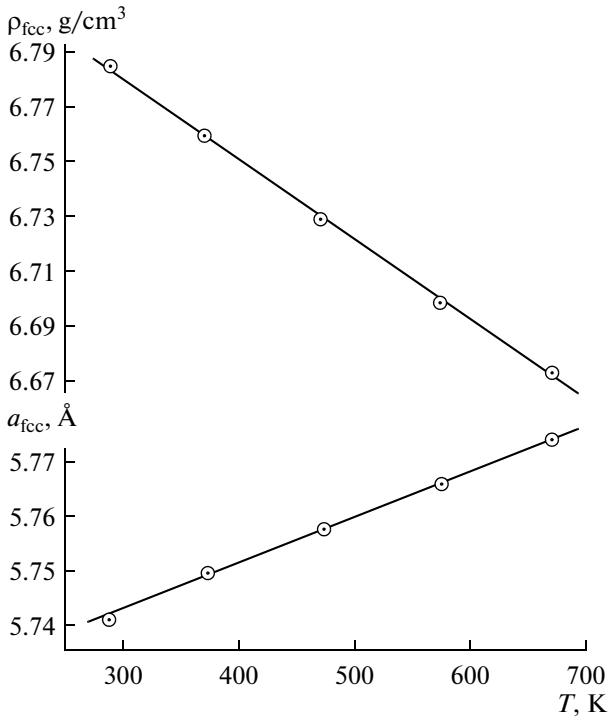

Fig. 9. Temperature dependence of the elementary cell parameters of the fcc $Cu_{1.75}Zn_{0.05}Se$ phase.

ture fcc modifications being metastable at room temperature [53].

It should be noted that both modifications are stable in the temperature interval of 290–873 K. Table 13 and Fig. 8 show the lattice parameters of both modifications calculated using diffraction data in a temperature interval of 290–873.

As one can see from Fig. 8, the lattice parameters of rhombic and fcc modifications increase linearly with temperature, while the density of these modifications linearly decreases. The density of the fcc modification is higher than that of rhombic modification, $\Delta\rho = \rho_{fcc} - \rho_{rhom} = 0.3$ g/cm^3.

Table 14 shows thermal expansion coefficients calculated using thermal dependence of lattice parameters. For the fcc lattice, thermal expansion coefficients along the basic crystallographic directions are equal: $\alpha_{[100]} = \alpha_{[010]} = \alpha_{[001]}$ and the surface of constant thermal expansion has a spherical shape with the highest symmetry $\frac{\infty}{\infty m}$.

In rhombic modification, all thermal expansion parameters are positive; the surface of constant thermal expansion has an ellipsoidal shape and the highest symmetry $\frac{m \cdot 2}{m}$.

9. STRUCTURAL ASPECTS OF THE POLYMORPHIC TRANSITIONS IN $Cu_{1.75}Zn_{0.05}Se$

For thermal and X-ray studies we used flat samples with dimensions of 5 × 4 × 2 mm (with arbitrary crystallographic orientation). At room temperature, the reflexes from (111), (200), (220), (311) and (400) planes corresponding to the cubic modification were registered in an angular interval of $10° \le 2\theta \le 70°$. These reflexes were also confirmed by the powder roentgenogram. After recording diffraction reflexes at room temperature, crystalline orientation was not altered and a URVT-200 oven was switched on for heating the samples. The corresponding thermal measurements of diffraction peaks were carried out in a temperature interval of 290–670 K. In this case we did not observe any changes in the number and intensity of

Table 13. Crystallographic parameters of $Cu_{1.80}Zn_{0.20}Se$ for different temperatures

T_{exp}, K	Modification	Lattice parameters			Z	Spatial group	V, Å^3	ρ, g/cm^3
		a, Å	b, Å	c, Å				
290	Orthorhombic	4.127	7.033	20.362	12	$P222_1$	591.011	6.957
	fcc	5.756			4	Fm3m	190.705	7.187
370	Orthorhombic	4.131	7.049	20.409	12	$P222_1$	594.298	6.919
	fcc	5.765			4	Fm3m	191.601	7.153
470	Orthorhombic	4.149	7.054	20.439	12	$P222_1$	598.189	6.875
	fcc	5.772			4	Fm3m	192.300	7.126
570	Orthorhombic	4.156	7.070	20.471	12	$P222_1$	601.498	6.836
	fcc	5.782			4	Fm3m	193.301	7.091
670	Orthorhombic	4.167	7.088	20.506	12	$P222_1$	605.659	6.790
	fcc	5.793			4	Fm3m	194.406	7.050
770	Orthorhombic	4.189	7.089	20.517	12	$P222_1$	609.269	6.749
	fcc	5.802			4	Fm3m	195.314	7.018
870	Orthorhombic	4.196	7.102	20.535	12	$P222_1$	611.943	6.720
	fcc	5.819			4	Fm3m	196.224	6.985

Table 14. Thermal expansion of the orthorhombic and fcc modifications of $Cu_{1.80}Zn_{0.20}Se$ crystal ($\times 10^6$ K^{-1})

T, K	$\alpha_{[100]}$	$\alpha_{[010]}$	$\alpha_{[001]}$	$\bar{\alpha} = \frac{\alpha_{[100]} + \alpha_{[010]} + \alpha_{[001]}}{3}$	$\beta = \alpha_{[100]} + \alpha_{[010]} + \alpha_{[001]}$
290–370	12.115	28.437	28.853	23.135	69.405
290–470	29.615	16.588	21.009	22.404	67.212
290–570	25.096	18.789	19.118	21.001	63.003
290–670	25.506	20.580	18.611	21.566	64.697
290–770	31.298	16.588	15.859	21.248	63.745
290–870	28.826	16.915	14.659	20.130	60.390
290–370	19.545			19.545	58.635
290–470	15.443			15.443	46.329
290–570	16.332			16.332	48.996
290–670	16.916			16.916	50.748
290–770	16.649			16.649	49.947
290–870	16.475			16.475	49.425

diffraction peaks. The lattice parameters and densities calculated according to these reflexes are presented in Table 15 and Fig. 9.

In the $Cu_{1.75}Zn_{0.05}Se$ crystalline structure, the Zn^{++} atoms occupy mainly the sites of Cu^{++} in tetrahedral voids. Mobilities of Zn^{++} atoms in $Cu_{1.75}Zn_{0.05}Se$ lattice and the bonds Zn–Se, Zn–Cu differ from the mobilities of Cu atoms in $Cu_{2-x}Se$, as well as from the bonds Cu–Se and Cu–Cu, which stabilize a high-temperature fcc modification [54].

Table 15. Period of the $Cu_{1.75}Zn_{0.05}Se$ lattice at 290–670 K

T_{exp}, K	Lattice period	Z	Spatial group	V, Å^3	ρ, g/cm^3
	a, Å				
290	5.741	4	Fm3m	189.218	6.787
370	5.749	4	Fm3m	190.010	6.759
470	5.758	4	Fm3m	190.904	6.728
570	5.766	4	Fm3m	191.701	6.698
670	5.774	4	Fm3m	192.500	6.673

Table 16. Thermal expansion of the fcc $Cu_{1.75}Zn_{0.05}Se$ crystal ($\times 10^6$ K^{-1})

T, K	$\alpha_{[100]}$	$\bar{\alpha} = \frac{3\alpha_{[100]}}{3}$	$\beta = 3\alpha_{[100]}$
290–370	17.419	17.419	52.257
290–470	16.451	16.451	49.353
290–570	16.552	15.552	46.656
290–670	16.127	15.127	45.381

Table 16 demonstrates the values of thermal expansion coefficients calculated from the temperature dependence of lattice parameters. In a cubic crystal, thermal expansion coefficients in three directions are equal and the corresponding surface of constancy have a spherical shape with the highest symmetry $\frac{\infty}{\infty m}$.

10. STRUCTURAL ASPECTS OF THE POLYMORPHIC TRANSFORMATIONS IN Ag_2Se

The α-Ag_2Se single crystals with a size of $5 \times 3 \times 1$ mm were installed on a diffractometer holder for flat samples. Seven distinct diffraction reflexes were recorded at room temperature in an angular interval of $10° \le 2\theta \le 90°$.

It is worth noting that powder roentgenograms and diffraction pictures recorded from single crystal are well reproduced in both structural models, namely $P222_1$ and $P2_12_12_1$. In what follows, we use the $P222_1$ structural model.

After recording diffraction reflexes at room temperature, a URVT-200 oven was switched on, and diffraction pictures at temperatures of 323, 373, and 393 K were recorded. We also did not find any changes in the number and intensity of diffraction peaks in this case. Having continued the sample heating up to 443 K, we found only three diffraction peaks in the former angular interval, corresponding to the (200), (211), and (210) planes in a high-temperature bcc modification. It was established that the temperature of equilibrium between α and β modifications is $T_{np} = 406 \pm 1$ K. This transformation is reversible and occurs between single crystal structures [55]. Table 17 and Fig. 10 give the calculated values of the lattice parameter and density of these modifications as a function of the temperature.

As we can see from Fig. 10, a microdensity changes abruptly under $\alpha \longrightarrow \beta$ transformation, and $\Delta\rho = \rho_\alpha - \rho_\beta = 0.18$ g/cm^3. This density difference increases elastic stresses at the boundary of these two modifications.

Figure 11 shows a series of micrographs for a low-temperature modification obtained for one and the same (110) face, corresponding to single crystals with β modification under the fivefold transformation. After $\beta_1 \longrightarrow \alpha_1$ transformation, the relief is clearly visible on this face (Fig. 11a). Figure 11b shows the same surface after grinding and polishing, while Fig. 11c demonstrates the result of elastic growth of α modification after the $\alpha_1 \longrightarrow \beta_2 \longrightarrow \alpha_2$ transformation. With further increase in the multiplicity of transformation, monocrystallinity sharply deteriorates due to accumulating the stresses and defects.

Using the thermal dependence of lattice parameters, thermal expansion coefficients were calculated for a low-temperature rhombic and for high-temperature bcc modifications of Ag_2Se. Table 18 shows the calculated thermal expansion coefficients.

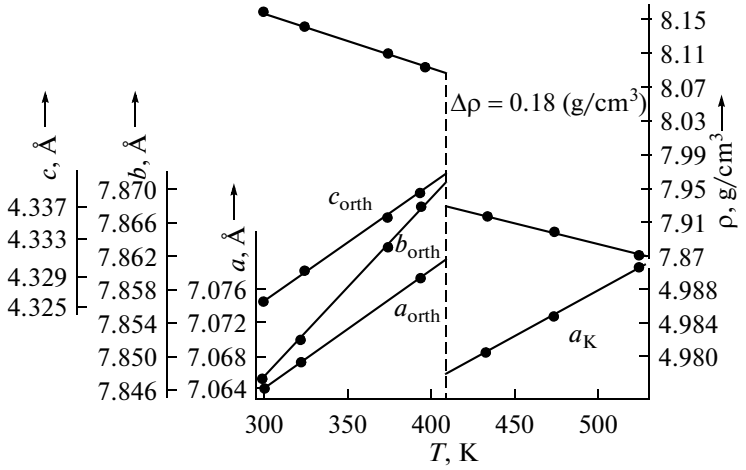

Fig. 10. Temperature dependence of the cell parameters and density for α- and β Ag_2Se crystalline modifications.

Table 17. Temperature dependence of the Ag_2Se lattice period

T_{exp}, K	Modification	Lattice parameters			Z	Spatial group	V, Å^3	ρ, g/cm^3
		a, Å	b, Å	c, Å				
299	Orthorhombic	7.065	7.847	4.325	4	$P222_1$	239.779	8.164
323	Orthorhombic	7.068	7.852	4.330	4	$P222_1$	240.261	8.145
373	Orthorhombic	7.074	7.863	4.336	4	$P222_1$	241.153	8.115
393	Orthorhombic	7.078	7.868	4.339	4	$P222_1$	241.598	8.100
433	fcc	4.981			2	Fm3m	12.573	7.918
473	fcc	4.985			2	Fm3m	123.849	7.901
523	fcc	4.991			2	Fm3m	124.296	7.872

As we can see from Table 18, for a rhombic Ag_2Se modification the thermal expansion coefficient slowly increases with increasing temperature in directions [100] and [010], and decreases in direction [001]. An anisotropic thermal expansion is one of the reasons for transforming a rhombic into the bcc modification with temperature.

11. POLYMORPHIC TRANSFORMATIONS IN AgCuSe

For diffraction studies, the specimens with dimensions of 4 × 4 × 1 mm were cut from the crystalline AgCuSe ingot with an arbitrary orientation at room temperature (295 K). In the angular interval of $10° \le 2\theta \le 90°$ 11 distinct diffraction reflexes were observed. These reflexes coincide with reflexes on a powder roentgenogram and they are accurately interpreted on the base of rhombic lattice parameters.

After recording diffraction pictures at room temperature, the oven was switched on and the test measurements were performed after each 50 K. The specimen temperature was kept constant for 40 min before the beginning of each recording. The previously recorded 11 diffraction patterns (at room temperature) did not vary up to a temperature of 495 K. At 545 K all these reflexes disappear and four new reflexes in the same angular interval are recorded with indexes (111), (200), (220), (311), which correspond to the high-temperature fcc modification with lattice parameters $a = 6.0823$ Å, $Z = 4$, spatial group Fm3m, and $\rho = 7.389$ g/cm^3 [56].

The temperature of equilibrium between modifications is $T = 504 \text{ K} \pm 1$ K. The transformations in AgCuSe are reversible and occur between single crystal structures.

Shown in Table 19 and Fig. 12 are the lattice parameters of the rhombic and fcc modifications calculated from diffraction picture. As one can see from Fig. 12, parameters a, b, c of the rhombic lattice and parameter a of the fcc modification increase linearly with temperature. The density of AgCuSe crystal decreases abruptly by $\Delta\rho = 0.28$ g/cm^3 when the rhombic modification is transformed to a high-temperature fcc modification [57].

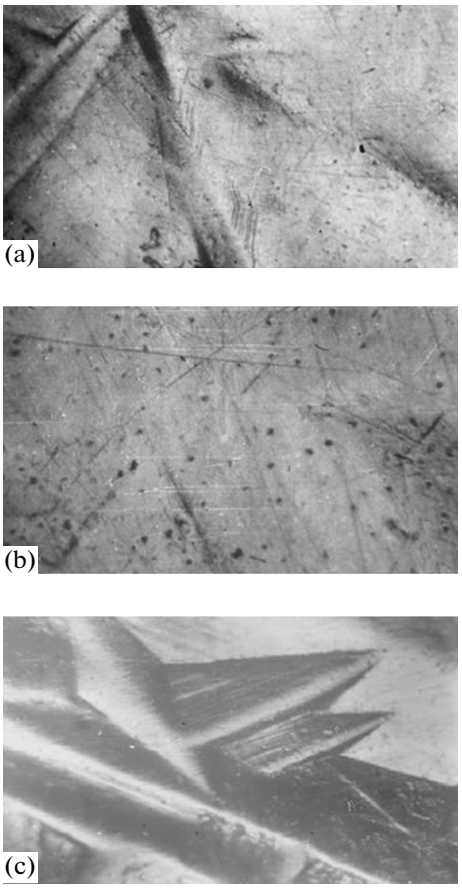

Fig. 11. Micrographs of the (110) face at a multiple $\alpha \rightleftharpoons \beta$ transformation in Ag_2Se. (a) micrograph of the (110) face of the β-modification after $\beta \longrightarrow \alpha_1$ transformation (elastic growth of the monoclinic low-temperature modification in the bcc crystalline matrix); (b) polished (110) face after $\beta \longrightarrow \alpha_1$ transformation; (c) micrograph of the same face after $\alpha_1 \longrightarrow \beta_1 \longrightarrow \alpha_2 \longrightarrow \beta_2$ transformation.

Table 18. Thermal expansion coefficients of the orthorhombic and bcc Ag_2Se crystalline modifications ($\times 10^6$ K^{-1})

T, K	$\alpha_{[100]}$	$\alpha_{[010]}$	$\alpha_{[001]}$	$\bar{\alpha} = \frac{\alpha_{[100]} + \alpha_{[010]} + \alpha_{[001]}}{3}$	$\beta = \alpha_{[100]} + \alpha_{[010]} + \alpha_{[001]}$
299–323	17.69	26.55	39.50	27.91	83.74
299–373	18.17	27.55	31.55	25.76	77.27
299–393	19.58	28.47	32.47	26.84	80.52
433–473	26.57			26.57	79.71
433–523	21.64			21.64	64.89

Table 19. Crystal parameters of the AgCuSe structures for different temperatures

T_{exp}, K	Modification	Lattice parameters			Z	Spatial group	V, Å^3	ρ, g/cm^3
		a, Å	b, Å	c, Å				
295	Orthorhombi	4.104	20.350	6.310	10	P4/nmm	526.988	7.888
345	Orthorhombi	4.111	20.412	6.321	10	P4/nmm	530.419	7.837
395	Orthorhombi	4.116	20.515	6.337	10	P4/nmm	535.095	7.768
445	Orthorhombi	4.125	20.565	6.349	10	P4/nmm	538.590	7.718
495	Orthorhombi	4.130	20.614	6.366	10	P4/nmm	541.975	7.669
504	fcc	6.069			4	Fm3m	223.538	7.436
545	fcc	6.082			4	Fm3m	224.978	7.389
595	fcc	6.097			4	Fm3m	226.646	7.334

Table 20 shows the thermal expansion coefficients calculated by using the temperature dependence of the rhombic and fcc modifications in a temperature interval of 295–595 K. For rhombic modification, the linear expansion coefficients along the [010] direction strongly differ from $\alpha_{[100]}$ and $\alpha_{[001]}$. From this it follows that the presence of thermal expansion anisotropy is mainly caused by the instability of a low-temperature AgCuSe modification.

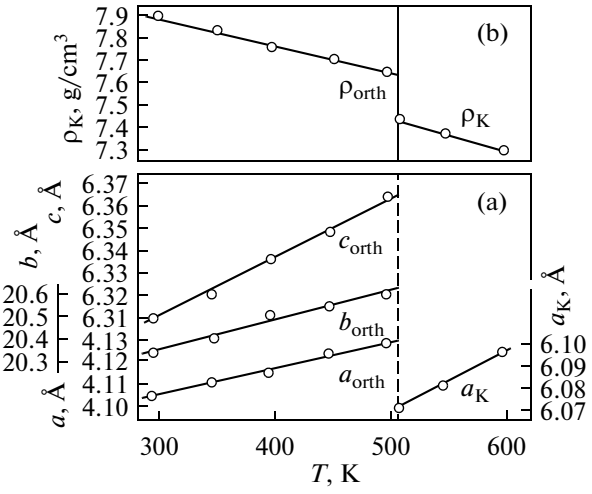

Fig. 12. Temperature dependence of the cell parameters (a) and density (b) for the orthorhombic and fcc AgCuSe crystalline modifications.

Crystallographic data and temperature of polymorphic transformations in binary Cu_2Se and Ag_2Se compounds are presented in Tables 9 and 17. As we can see, the transition temperatures between a low-temperature rhombic modification and high-temperature fcc/bcc modifications (Cu_2Se and Ag_2Se) are equal. In a ternary AgCuSe alloy, i. e. $1/2(Cu_2Se \cdot Ag_2Se)$, the temperature of equilibrium between the low-temperature rhombic and high-temperature fcc modification is by 96 K higher than in the Cu_2Se and Ag_2Se binary alloys.

It is worth noting that the lattice parameters of a low-temperature rhombic AgCuSe and Cu_2Se modifications are nearly equal. In the Cu_2Se crystal lattice, Cu atoms are statistically distributed in tetrahedral positions formed by Se atoms. In AgCuSe structure, Ag atoms are located in the planes perpendicular to the c axis, while Cu atoms, similarly to a Cu_2Se structure, are located in the center of tetrahedrons formed by Se atoms. These structural differences and the formation of additional Cu–Ag and Ag–Se atomic bonds also cause the growth of transition temperature in AgCuSe (T_{np} = 504 K) as compared to Cu_2Se (T_{np} = 407 K) and Ag_2Se (T_{np} = 408 K).

Table 20. Thermal expansion coefficients of the orthorhombic and fcc AgCuSe crystal modifications ($\times 10^6$ K^{-1})

T, K	$\alpha_{[100]}$	$\alpha_{[010]}$	$\alpha_{[001]}$	$\bar{\alpha} = \frac{\alpha_{[100]} + \alpha_{[010]} + \alpha_{[001]}}{3}$	$\beta = \alpha_{[100]} + \alpha_{[010]} + \alpha_{[001]}$
295–345	34.113	60.934	34.865	43.304	129.912
295–395	29.240	81.081	42.789	51.037	153.110
295–445	34.113	70.434	41.204	48.584	145.751
295–495	31.676	64.865	44.374	46.972	140.915
504–545	52.245			52.245	156.735
504–595	50.699			50.699	152.097

Table 21. Same as in Table 19 for $Ag_{0.4}Cu_{1.6}Se$ structures

T_{exp}, K	Modification	Lattice parameters			Z	Spatial group	V, Å^3	ρ, g/cm^3
		a, Å	b, Å	c, Å				
293	AgCuSe–orthorhombic	4.104	20.350	6.310	10	P4/nmm	526.988	7.885
	Ag_2Se–orthorhombic	4.333	7.062	7.764	4	$P2_12_12_1$	237.576	8.237
373	AgCuSe–orthorhombic	4.105	20.396	6.318	10	P4/nmm	528.978	7.858
	Ag_2Se–orthorhombic	4.340	7.089	7.765	4	$P2_12_12_1$	238.900	8.192
473	AgCuSe–orthorhombic	4.120	20.453	6.301	10	P4/nmm	530.962	7.828
	Ag_2Se–orthorhombic	4.361	7.126	7.773	4	$P2_12_12_1$	241.558	8.101
523	AgCuSe–orthorhombic	4.153	20.533	6.312	10	P4/nmm	538.247	7.723
	Ag_2Se–orthorhombic	4.424	7.172	7.759	4	$P2_12_12_1$	246.185	7.949
573	$Ag_{0.4}Cu_{1.6}Se$–fcc	5.896			4	Fm3m	204.962	7.250
673	$Ag_{0.4}Cu_{1.6}Se$–fcc	5.903			4	Fm3m	205.692	7.223

12. STRUCTURAL ASPECTS OF POLIMORPHIC TRANSFORMATIONS IN $Ag_{0.4}Cu_{1.6}Se$

For diffraction investigations, the specimens with dimensions of $2 \times 4 \times 6$ mm were cut at room temperature. 18 distinct diffraction patterns were observed in an angular interval of $10° \le 2\theta \le 110°$. 14 of these reflexes are interpreted on the base of the parameters of AgCuSe rhombic modification, whereas the remaining four and seven of those 14 reflexes are interpreted on the base of Ag_2Se rhombic modification. From this it follows that $Ag_{0.4}Cu_{1.6}Se$ and $Ag_{1.5}Cu_{0.5}Se$ crystals are two-phase at room temperature.

After diffraction picture recording at room temperature, the oven was switched on and test measurements were performed after each 50 K. The specimen temperature was kept constant for 50 min before the beginning of each recording.

We did not observe the changes in the number and intensity of diffraction patterns in a temperature interval of 293–523 K. At 573 K, all diffraction reflexes disappear and seven new reflexes are observed in the former angular interval corresponding to a high-temperature modification with lattice parameter a = 5.896 Å [58].

In Table 21 and Fig. 12, the temperature dependences of lattice parameters for both rhombic and fcc $Ag_{0.4}Cu_{1.6}Se$ modifications are given. As we can see from Fig. 13, parameters of the modified AgCuSe structure sharply differ from linearity and from a and b parameters for Ag_2Se modification.

Table 22 shows that thermal expansion parameters of the AgCuSe rhombic modification are positive in all basic crystallographic directions. The thermal expansion parameters of a rhombic modification at 523 K satisfy conditions $\alpha_{[100]}, \alpha_{[010]} > 0$, $\alpha_{[001]} < 0$, i.e. in this case there is one elongated positive region and two ellipsoidal negative regions (if we have one negative thermal expansion parameter). From this it follows that thermal expansion is one of the reasons of instability for a low-temperature crystalline modification.

13. STRUCTURAL ASPECTS OF THE POLIMORPHIC TRANSFORMATIONS IN $Ag_{1.5}Cu_{0.5}Se$

We recorded 27 diffraction reflexes at room temperature in an angular interval of $10° \le 2\theta \le 90°$ for $Ag_{1.5}Cu_{0.5}Se$ polycrystalline sample in the form of the plate with dimensions of $4 \times 5 \times 1$ mm. For exact

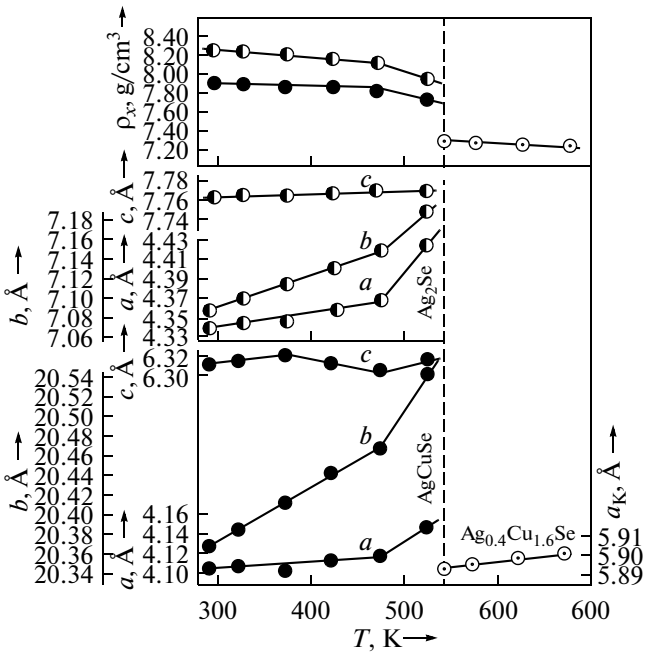

Fig. 13. Temperature dependence of the cell parameters, volume, and density for the orthorhombic and fcc $Ag_{0.4}Cu_{1.6}Se$ crystalline modifications. (●) parameters *a, b, c* of crystal lattice and density for $Ag_{0.4}Cu_{1.6}Se$; (◑) parameters *a*, *b*, *c* of crystal lattice and density for Ag_2Se; (⊙) parameter *a* and density ρ_x for the fcc $Ag_{0.4}Cu_{1.6}Se$ modification. The calculated thermal expansion coefficients for the modifications present in $Ag_{0.4}Cu_{1.6}Se$ obtained by using the temperature dependence of lattice parameters are given in Table 21.

indexing of these diffraction data, experimental interplanar distances d_i in $Ag_{1.5}Cu_{0.5}Se$ were compared to the corresponding values calculated on the base of crystal lattice parameters of low-temperature AgCuSe, Cu_2Se, and Ag_2Se modifications. Except the values $d = 2.4812$ Å and $d = 1.8625$ Å, experimental values of d_i for $Ag_{1.5}Cu_{0.5}Se$ are in a satisfactory agreement with calculated parameters $a = 4.333$ Å, $b = 7.062$ Å, $c = 7.764$ Å for Ag_2Se. The aforementioned two interplanar distances, as well as others, are indexed on the base of elementary cell parameters of a low-temperature AgCuSe rhombic modification with lattice parameters $a = 4.105$ Å, $b = 20.350$ Å, and $c = 6.310$ Å.

Up to a temperature of 423 K, there are no changes in the diffraction patterns recorded at room temperature. At 423 K, 14 reflexes are observed in the same angular range of the two-phase state. At 488 K all reflexes disappear and four new reflections are observed with (200), (220), (311), and (400) indexes, which are characteristic for a high-temperature fcc modification with elementary cell parameter $a = 6.107$ Å [58, 59].

At room temperature, the two-phase $Ag_{1.5}Cu_{0.5}Se$ samples look like a single-phase with the structure of a high-temperature AgCuSe modification. In another case, a rhombic low-temperature Ag_2Se modification would be transformed into the bcc structure at a temperature of 406 K, whereas the AgCuSe rhombic modification would be transformed to the fcc structure at a temperature of 504 K. Consequently, at temperatures higher than 504 K the sample would consist of the bcc and fcc phases.

Table 23 gives the temperature dependence of lattice parameters for these and fcc modifications in a temperature interval of 295–573 K; Fig. 14 shows these results graphically. As one can see from Fig. 14, the parameters *a* and *c* for Ag_2Se and the value of *a* for AgCuSe increase linearly with temperature, whereas parameter *b* for Ag_2Se and parameters *b*, *c* for CuAgSe deviate from linearity. Thermal expansion coefficients for both rhombic and fcc $Ag_{1.5}Cu_{0.5}Se$ modifications calculated using the thermal dependence of lattice parameters are listed in Table 24.

14. STRUCTURAL ASPECTS OF THE POLIMORPHIC TRANSFORMATIONS IN $AgCuSe_{0.5}S_{0.5}$

We registered 16 diffraction reflexes from randomly oriented $AgCuSe_{0.5}S_{0.5}$ crystal with dimensions of 1 × 5 × 5 mm in an angular interval of $10° \le 2\theta \le 100°$. Indexing of these phases indicates the presence of two phases in the sample, one of which is identical to a

Table 22. Same as in Table 20 for $Ag_{0.4}Cu_{1.6}Se$

T, K	$\alpha_{[100]}$	$\alpha_{[010]}$	$\alpha_{[001]}$	$\bar{\alpha} = \frac{\alpha_{[100]} + \alpha_{[010]} + \alpha_{[001]}}{3}$	$\beta = \alpha_{[100]} + \alpha_{[010]} + \alpha_{[001]}$
293–373	3.046	28.256	15.848	15.717	47.150
293–473	21.659	28.119	7.924	19.234	57.702
293–523	51.911	39.098	1.378	30.796	92.387
293–373	20.194	47.791	1.610	23.198	69.595
293–473	35.900	50.348	6.440	30.896	92.686
293–523	91.311	67.723	−2.800	52.078	156.234
523–673	11.872			11.872	35.616

Table 23. Same as in Table 17 for $Ag_{1.5}Cu_{0.5}Se$

T_{exp}, K	Modification	Lattice parameters			Z	Spatial group	V, Å^3	ρ, g/cm^3
		a, Å	b, Å	c, Å				
295	Ag_2Se—orthorhombic	4.333	7.062	7.764	4	$P2_12_12_1$	237.576	8.237
	AgCuSe—orthorhombic	4.105	20.350	6.310	10	P4/nmm	527.117	7.885
373	Ag_2Se—orthorhombic	4.340	7.084	7.787	4	$P2_12_12_1$	239.408	8.175
	AgCuSe—orthorhombic	4.110	20.481	6.307	10	P4/nmm	530.904	7.829
423	Ag_2Se—orthorhombic	4.354	7.068	7.869	4	$P2_12_12_1$	242.161	8.119
	AgCuSe—orthorhombic	4.085	20.797	6.317	10	P4/nmm	536.665	7.744
473	Ag_2Se—orthorhombic	4.364	7.078	7.900	4	$P2_12_12_1$	244.013	8.019
	AgCuSe—orthorhombic	4.090	20.793	6.330	10	P4/nmm	538.325	7.721
523	fcc	6.107			4	Fm3m	227.753	7.950
573	fcc	6.118			4	Fm3m	228.936	7.900

low-temperature $Cu_{1.96}S$ monoclinic lattice with parameters $a = 26.897$ Å, $b = 15.515$ Å, $c = 13.585$ Å, $\beta = 90.13°$, $Z = 128$, spatial group $P2_1/n$, $\rho = 5.870$ g/cm^3, and another one has the elementary cell of the low-temperature AgCuSe rhombic lattice [60].

After recording diffraction pictures at room temperature, the oven was switched on and the test measurements were performed after each 100 K. The specimen orientation was not changed. The number of reflexes and their intensity recorded at room temperature also did not vary with increasing temperature. But at 773 K, we found 9 reflexes in the same angular interval corresponding to a high-temperature fcc modification with elementary cell parameter $a = 6.356$ Å, $Z = 4$, and spatial group Fm3m. It was established that the equilibrium temperature between the low-temperature and high-temperature modifications is $T = 695$ K.

Using this diffraction picture, we calculated the elementary cell parameters for the $AgCuSe_{0.5}S_{0.5}$ crystal in a temperature interval of 293–973 K (Table 25 and Fig. 15).

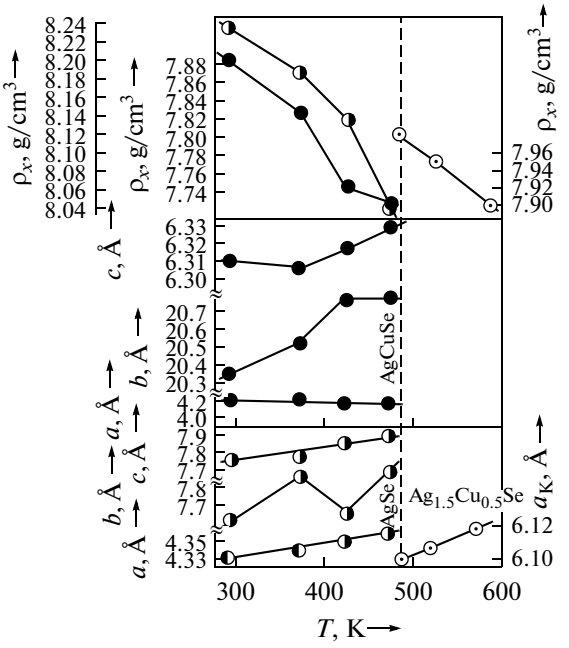

Fig. 14. Temperature dependence of the cell parameters and density for $Ag_{1.5}Cu_{0.5}Se$ modifications. (●) parameters a, b, c of crystal lattice and density for AgCuSe; (◑) parameters a, b, c of crystal lattice and density for Ag_2Se; (⊙) parameter a and density ρ_x for the fcc $Ag_{1.5}Cu_{0.5}Se$

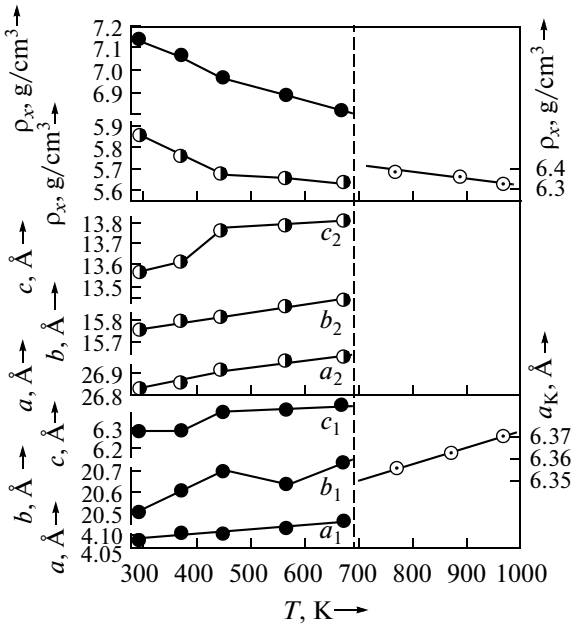

Fig. 15. Temperature dependence of the cell parameters of the phases present in $AgCuSe_{0.5}S_{0.5}$. (●) parameters a_1, b_1, c_1 of lattice and the densities of the orthorhombic AgCuSe phase; (◑) parameters a_2, b_2, c_2 and the densities of the monoclinic $Cu_{1.6}S$; (⊙) parameter a and density of the fcc modification.

Table 24. Same as in Table 18 for $Ag_{1.5}Cu_{0.5}Se$ ($\times 10^6$ K^{-1})

Modification	T, K	$\alpha_{[100]}$	$\alpha_{[010]}$	$\alpha_{[001]}$	$\bar{\alpha} = \frac{\alpha_{[100]} + \alpha_{[010]} + \alpha_{[001]}}{3}$	$\beta = \alpha_{[100]} + \alpha_{[010]} + \alpha_{[001]}$
Ag_2Se	295–373	19.04	39.65	36.71	31.80	95.40
	295–473	37.28	5.99	103.8	49.03	147.10
	295–473	40.13	12.67	3	49.92	149.76
				96.96		
AgCuSe	295–373	15.23	80.34	–6.14	29.81	89.43
	295–423	37.48	169.08	8.53	71.70	215.09
	295–473	33.56	120.88	17.26	57.23	171.70
fcc	523–573	37.99			37.99	113.97

Table 25. Temperature dependence of the lattice parameters for $AgCuSe_{0.5}S_{0.5}$ crystal modifications

T_{exp}, K	Modification	Lattice parameters			β	Z	Spatial group	V, Å^3	ρ, g/cm^3
		a, Å	b, Å	c, Å					
293	$Cu_{1.96}S$–monoclinic	26.827	15.745	13.565	90.13°	8	$P2_1/n$	5729.735	5.807
	AgCuSe–orthorhombic	4.086	20.524	6.279		10	P4/nmm	526.564	7.154
373	$Cu_{1.96}S$–monoclinic	26.867	15.794	13.611	90.13°	8	$P2_1/n$	5775.656	5.761
	AgCuSe–orthorhombic	4.103	20.615	6.288		10	P4/nmm	531.860	7.083
473	$Cu_{1.96}S$–monoclinic	26.913	15.811	13.763	90.13°	8	$P2_1/n$	5856.452	5.682
	AgCuSe–orthorhombic	4.135	20.699	6.373		10	P4/nmm	545.467	6.906
573	$Cu_{1.96}S$–monoclinic	26.948	15.847	13.782	90.13°	8	$P2_1/n$	5885.534	5.654
	AgCuSe–orthorhombic	4.138	20.681	6.388		10	P4/nmm	546.672	6.891
673	$Cu_{1.96}S$–monoclinic	26.971	15.884	13.804	90.13°	8	$P2_1/n$	5913.735	5.627
	AgCuSe–orthorhombic	4.163	20.743	6.393		10	P4/nmm	552.055	6.824
773	fcc	6.356				4	Fm3m	253.774	6.376
873	fcc	6.363				4	Fm3m	257.624	6.355
973	fcc	6.372				4	Fm3m	258.718	6.328

As we can see from Fig. 15, parameters a_2, b_2, c_2 of the $Cu_{1.96}Se$ monoclinic lattice nonlinearly vary when the temperature is higher than 373 K. Parameter a_2 diminishes up to a temperature of 373 K and linearly increases at higher temperatures. Parameters a_1 and c_1 of a rhombic AgCuSe structure vary nonlinearly.

Despite such behavior of the lattice parameters for both modifications in dependence of temperature, there are no considerable changes in the number of diffraction reflexes and intensities.

It should be noted that the layers of sulfur atoms form a hexagonal dense-packing structure in a low-temperature monoclinic $Cu_{1.96}S$ lattice; the copper atoms are distributed between these layers in distorted triangles, nine of them being in tetrahedral positions and one atom has two nearest neighbors. It is also possible that silver atoms partially occupy the sites of copper atoms.

In the lattice AgCuSe, Ag atoms are in the planes perpendicular to the c axis. Each of them has four Ag atoms at a distance of 2.96 Å and six sulfur atoms at distances of 2.67 Å (four atoms), 3.59 Å (one atom), and 3.64 Å (one atom). Sulfur atoms form elongated tetrahedrons in which Cu atoms are located. The Se–Se distances are equal to 3.30 Å, the distances Cu–Se vary from 2.06 Å to 2.50 Å, and the minimum Cu–Ag distance is 2.98 Å.

At room temperature, the $AgCuSe_{0.5}S_{0.5}$ crystals consist of the two phases and deform one another with increasing temperature. A nucleation center of the fcc modification is formed at the boundary of these phases, and starts growing upon the presence of two phases. Two phases are formed when cooling a single fcc crystal, i. e. the crystal returns to its primary state. The transformations "single crystal–single crystal" are reversible.

Table 26. Same as in Table 18 for $AgCuSe_{0.5}S_{0.5}$ ($\times 10^6$ K^{-1})

Composition	T, K	$\alpha_{[100]}$	$\alpha_{[010]}$	$\alpha_{[001]}$	$\bar{\alpha} = \frac{\alpha_{[100]} + \alpha_{[010]} + \alpha_{[001]}}{3}$	$\beta = \alpha_{[100]} + \alpha_{[010]} + \alpha_{[001]}$
$Cu_{1.96}S$	293–373	18.638	38.901	42.388	33.309	99.927
	293–473	17.810	23.288	81.091	40.730	122.189
	293–573	16.109	23.137	57.132	32.126	96.378
	293–673	14.126	23.232	46.365	27.908	83.723
AgCuSe	293–373	52.007	55.423	17.917	41.782	125.347
	293–473	66.623	47.370	83.170	65.721	197.163
	293–573	45.451	27.320	61.998	44.923	134.769
	293–673	49.592	28.080	47.778	41.817	125.450
fcc	773–873	11.013			11.013	33.039
$AgCuSe_{0.5}S_{0.5}$	773–973	12.587			12.587	37.761

The calculated thermal expansion coefficients obtained using thermal dependence of the lattice parameters of $AgCuSe_{0.5}S_{0.5}$ modifications are listed in Table 26.

As we can see from Table 26, for the structure of $Cu_{1.96}S$ thermal expansion coefficients in the [010] direction significantly differ from those in the [100] and [001] directions, i. e. $\alpha_{[100]} < \alpha_{[010]} > \alpha_{[001]}$. Whence it follows that the thermal expansion anisotropy is one of the reasons of polymorphism in $AgCuSe_{0.5}S_{0.5}$.

15. STRUCTURAL ASPECTS OF POLYMORPHIC TRANSFORMATIONS IN $AgCuSe_{0.5}Te_{0.5}$

At room temperature, we recorded 22 diffraction reflexes from a 1 × 5 × 5 mm $AgCuSe_{0.5}Te_{0.5}$ crystal with arbitrary orientation within an angular interval of $10° \le 2\theta \le 90°$, which coincide with reflexes on a powder roentgenogram of the synthesized sample. The $AgCuSe_{0.5}Te_{0.5}$ sample consists of three phases: phase **I** is identical to the low-temperature rhombic Cu_2Te phase with crystal lattice parameters $a = 7.319$ Å, $b = 22.236$ Å, $c = 36.458$ Å; phase **II** is crystallized in a rhombic structure of a low-temperature CuAgSe phase; and **III** is the cubic phase with a diamond-like structure and lattice parameter $a = 7.319$ Å [16].

Most of reflexes from these phases on the diffractogram are superimposed. A multiphase structure of the $AgCuSe_{0.5}Te_{0.5}$ composition is caused mainly by the redistribution of Se and Te anions and Ag and Cu cations, respectively. After recording X-ray pattern at room temperature, the oven was switched on and the test recordings were performed after each 50 K. The sample temperature was kept constant during 40 min before the beginning of each recording. At these conditions, the $AgCuSe_{0.5}Te_{0.5}$ sample is in a triple-phase state and both rhombic phases are reversibly transformed into a cubic phase at 444 ± 1 K.

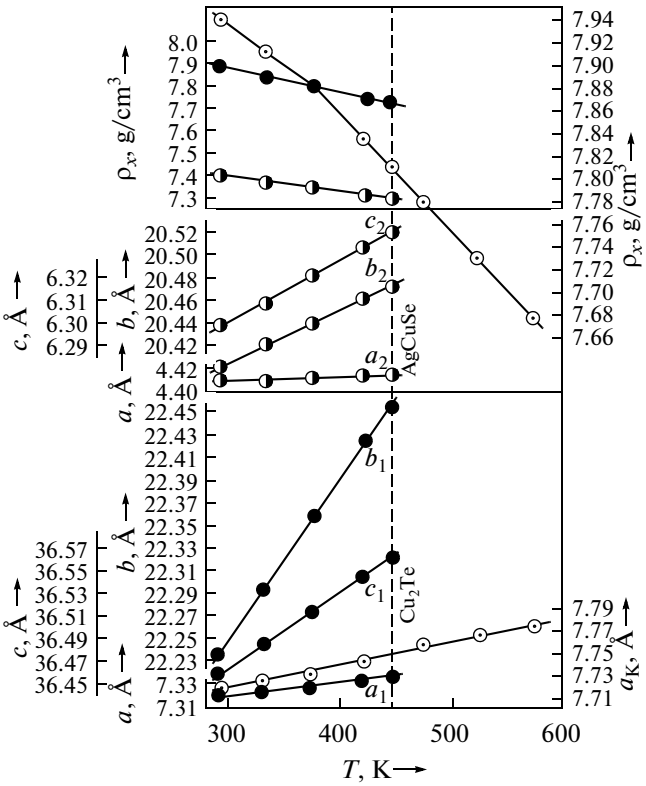

Fig. 16. Same as in Fig. 15 for $AgCuSe_{0.5}Te_{0.5}$. (●) parameters a_1, b_1, c_1 of lattice and densities of the orthorhombic Cu_2Te phase; (◑) parameters a_2, b_2, c_2 and densities for monoclinic AgCuSe; (⊙) parameter a and the density for cubic modification.

Table 27. Same as in Table 25 for $AgCuSe_{0.5}Te_{0.5}$

T_{exp}, K	Modification	Lattice parameters			Z	Spatial group	V, Å^3	ρ, g/cm^3
		a, Å	b, Å	c, Å				
293	Cu_2Te–orthorhombic	7.319	22.236	36.458	104	P6/mmm	5933.358	7.41
	AgCuSe–orthorhombic	4.107	20.421	6.299	10	P4/nmm	528.291	8.00
	AgCuSe–cubic	7.715			8	Fd3m	459.205	7.94
373	Cu_2Te–orthorhombic	7.329	22.361	36.515	104	P6/mmm	5984.216	7.36
	AgCuSe–orthorhombic	4.110	20.442	6.322	10	P4/nmm	531.153	7.82
	AgCuSe–cubic	7.729			8	Fd3m	461.711	7.90
473	$AgCuSe_{0.5}Te_{0.5}$–cubic	7.759			8	Fd3m	467.108	7.81

The lattice parameters of coexisting phases calculated using X-ray picture are shown in Table 27 and Fig. 15, As one can see, the lattice parameters of rhombic and cubic modifications increase linearly with temperature. Moreover, it should be noted that the lattice parameter of a cubic phase linearly depends on temperature when both rhombic phases are transformed into a cubic phase. It follows that under this phase transition the role of precursor is played by a cubic phase.

CONCLUSIONS

In conclusion, we note that the ranges of coexistence of separate crystalline modifications of certain compositions from room temperature to the melting point were determined using a high-temperature X-ray diffractometry. It is shown that, irrespective of the type of structure and chemical bonds, the transition from one crystalline structure to another occurs with the formation and growth of a nucleation center in the crystal with new modification inside the crystalline matrix. Similarity of structures or structural elements in the bulk and the densities of both modifications favor the conditions of transformation from one crystalline phase to another.

REFERENCES

1. M. Khansen and K. Anderko, *Structures of Binary Alloys* (Metallurgizdat, Moscow, 1963) [in Russian].
2. F. Shank, *Structures of Binary Alloys* (Metallurgizdat, Moscow, 1973) [in Russian].
3. D. M. Chizhikov and V. A. Schastlivyi, *Selen and Selenides* (Nedra, Leningrad, 1968) [in Russian].
4. P. Rahlfs, "Uber die Kubischen Hochtempertur Modificationen der Sulfide, Selenide und Telluride des Silbers und des einwertingen Kupfers," Z. Phys. Chem. B **31**, 157–194 (1936).
5. L. Gulay, M. Daszkiewicz, O. Strok, and A. Pietraszko, "Crystal structure of Cu_2Se," Chem. Met. Alloys **4**, 200 (2011).
6. X. Shi, F. Xu, L. Zhang, W. Zhang, L. Chen, Q. Li, C. Uher, T. Day, and G. J. Snyder, "Copper ion liquid-like thermoelectrics," Nature Materials **11**, 422 (2012).
7. W. Borchert, "Gitterumwandlungen im system $Cu_{2-x}Se$," Z. Kristallogr. **106**, 5–24 (1945).
8. P. Junod, "Relations entre la structure cristalline et les propriétés electroniques des combinaisons Ag_2S, Ag_2Se, Cu_2Se," Helv. Phys. Acta **32**, 567–571 (1959).
9. I. W. Earley, "Description and synthesis of selenides minerals," Am. Mineral. **35** (5–6), 337–364 (1950).
10. N. A. Ibragimov, "Influence of uniaxial deformation on physical properties of Cu_2S and Cu_2Se," Candidate's Dissertation in Mathematics and Physics (Baku, 1985).
11. V. A. Kotovich and V. D. Frank-Kotenskii, Uch. Zap. LGU, Ser. Geol. **8**, 1356 (1957).
12. A. L. N. Stevels and F. Jellinek, "Phase transitions in copper chalgogenides-I. The copper-selenium system," Rec. Truv. Chem. **90** (3), 273–279 (1971).
13. M. Bellati and S. Lussana, "Azione della luce sulla conducibilita calorißca del selenio crislaliino," Atti H. Islit. Veneto d. Sc. Ictl. ed arti, (6), 6 (1887); HH-H 35. Ausz. Z. **14**, 505–525 (1987).
14. S. K. Sharma, "Structural transformation in thin films of binary alloys," J. Mater. Sci. **4** (3), 541–546 (1969).

15. R. D. Heyding, "The copper-selenium system," Can. J. Chem. **44** (10), 1233–1249 (1966).

16. Yu. G. Asadov, A. G. Babayev, Yu. I. Aliyev, F. G. Magerramova, and R. J. Aliyeva, "Thermal extensions and polymorphous transitions in $Cu_{2-x}A_xSe$ (x = 0; 0.2; 0.4, A = Ag, Zn), CuAgSe, $CuAgSe_{0.5}(S,Te)_{0.5}$ crystals," Azerb. J. Phys. Fizika. **15** (4), 89 (2009).

17. W. Hartwing, "The crystal structure of berzelanite (Cu_2Se)," J. Mineral **4**, 83–87 (1972).

18. O. S. Klymovych, O. F. Zmiy, L. D. Gulay, and T. A. Ostapyuk, "Phase diagram of the $Ag2Se–As_2Se_3$ system and crystal structure of the $AgAs_3Se_5$ compound," Chem. Met. Alloys **1**, 288–292 (2008).

19. J. Yu and H. Yun, "Reinvestigation of the low-temperature form of Ag_2Se (Naumannite) based on single-crystal data," Acta Cryst. E **67** (2011).

20. L. S. Ramsdell, "The crystallography of acanthine, Ag_2S," Am. Mineral. **28**, 401–425 (1943).

21. A. Boettcher, S. Hasse, and H. Treupel, "The structures and structural changes in the sulfides and selenides of silver and copper," Z. Angew. Phys. **7**, 478–487 (1955).

22. L. W. Constantinesch and A. Ichimesku, "L'etude des conditions d'obtention des couches orientees α-Ag_2Se," Rev. Poum. Phys. **18** (10), 1197–1201 (1973).

23. L. W. Constantinesch, "Electron effective mass in the low temperature phase of silver selenides thick films," Thin Solid Films **28** (1), 73–79 (1983).

24. De R. Ridder and S. Amelinckx, "An electron microscopy study of the polymorphic transformation in Ag_2Se (I)," Phys. Stat. Sol. A **18**, 99–110 (1973).

25. Y. Saito and M. Sato, "Orientation in Ag_2Se polymorphic films produced by the reaction of silver films with selenium," Thin Solid Films **79**, 259–266 (1981).

26. Y. Beer, G. Buseh, and C. Prohlich, "Warmeleit Faigkeit Electrische Leifahigeit. Hall-effect Termospanninung und Spezifische Woirme van Ag_2Se," Z. Naturforsch., A: Phys. Sci. **1701**, 886–898 (1962).

27. P. Junod, "Relations entre la Structure Cristalline et les Proprietes Electroniques des combinaisons Ag_2S, Ag_2Se, Cu_2Se," Helv. Phys. Acta **32** (6–7), 567–577 (1959).

28. N. Nuruev and R. Sharifzade, "On the conditions of formation and stability of tetragonal Ag_2Se modification," Neorg. Mater. **2**, 73–78 (1972).

29. W. Klemm, H. Sodomann, and P. Langmesser, "Beitrage zur Kenntnis der Alkalimetallchalkogenide," Z. Anorg. Allgem. Chem. **241**, 281–293 (1939).

30. L. B. Conn and R. G. Taylor, "Thermoelectric and crystallographic properties of Ag_2Se," J. Electrochem. Soc. **107**, 977–986 (1960).

31. Ts. L. Chzhou and Z. G. Pinsker, "Electron diffraction studies of thin AgSe films," Crystallography, **7**, 66–71 (1962).

32. R. Simon, "Preparation and thermoelectric properties of β-Ag_2Se," Adv. Energy Convers. **3**, 481–505 (1963).

33. A. Novoselova, "Studying the silver selenide–lead selenide system," Izv. Acad. Nauk SSSR, Neorg. Mater. **3**, 1010–1019 (1967).

34. S. K. Sharma and C. A. Wiegers, "The crystal structure of the low-temperature form of silver selenides," Am. Mineral. **56**, 1882 (1971).

35. N. G. Dhere and A. Goswami, "Growth of vapour phase deposits of Ag_2Se and Ag_2Te on single crystals," Thin Solid. Films **5** (3), 137–144 (1970).

36. C. A. Wiegers, "The crystal structure of the low-temperature form of silver selenides," Am. Mineral. **56**, 1882–1898 (1971).

37. Yu. G. Asadov and G. A. Jabrailova, "Investigation of polymorphic transformations in Ag_2Se," Phys. Stat. Sol. (a) **12** K13 (1972).

38. S. A. Aliev, *Diffuse Phase Transitions in Semiconductors and High-Temperature Superconductors* (Elm, Baku, 2007) [in Russian].

39. J. R. Cunter, N. Uyeda, and E. Suito, "Topotactic reaction of thin silver films with selenium," J. Cryst. Growth **33**, 337–352 (1973).

40. M. D. Banus, "Pressure dependence of the alpha-beta transition temperature silver selenides," Science **147**, 732–746 (1965).

41. S. K. Sharma and G. L. Malhota, "Some observations on structural transformation of Ag_2Se alloy films," Phys. Lett. **9**, 218 (1964).

42. M. N. Agaev, Sh. M. Alekperova, and M. I. Zargarova, "Physico-chemical studying of the system $Ag_2Te–Cu_2Te$," Dokl. Akad. Nauk Azerb. SSR **27** (6), 15 (1971).

43. D. M. Trots, A. N. Skomorokhov, M. Knapp, and H. Fuess, "High-temperature behaviour of average structure and vibrational density of states in the ternary superionic compound AgCuSe," Eur. Phys. J. B **51**, 507–511 (2006).

44. D. M. Trots, A. N. Skomorokhov, and M. Knapp, "High-temperature behaviour of average structure and vibrational density of states in the ternary superionic compound AgCuSe," Eur. Phys. J. B **51**, 507–512 (2006).

45. V. N. Chebotin, V. N. Konev, and V. M. Berezin, "Chemical diffusion in nonstoichiometric solid solutions ($(Cu_{1-x}Ag_{x+6})_{2x}$, where x = Se, S)," Neorg. Mater. **20** (9), 1662–1465 (1984).

46. R. A. Yakshybaev, N. N. Mukhammadeva, and V. N. Kopev, "Studying the phase states in $Cu_2Se–Ag_2Se$ quasibinary system using high-temperature radiography," in *Abstr. III-rd All-Union Meeting on Chemistry and Technology of Chalcogenides and Chalcogenes* (Karaganda, 1986), p. 269.

47. W. J. Earley, "Description and synthesis of selenides minerals," Am. Mineral. **35** (5–6), 345–364 (1950).

48. A. J. Frueh, G. K. Czamanste, and Ch. Knight, "The crystallography of eucairite, AgCuSe," Zeit. Krist. **108**, 389–396 (1957).

49. Yu. G. Asadov and G. A. Jabrailova, "Investigation of structural transformations in Cu_2Se," Cryst. and Tech. **8** (4), 509 (1973).

50. M. Kh. Balapanov, R. A. Yakshibaev, and U. Kh. Mukhamed'yanov, "Phenomena of ion transport in solid solutions of superionic conductors Cu_2Se and Ag_2Se," Phys. Solid State **45** (4), 634–638 (2003).

51. S. A. Danilkin, A. N. Skomorokhov, A. Hoser, H. Fuess, V. Rajevac, and N. N. Bickulova, "Crystal structure and lattice dynamics of superionic copper selenide $Cu_{2-\delta}Se$," J. All. Comp. **361** (1), 57–61 (2003).

52. Yu. G. Asadov, G. A. Dzhabrailova, and V. I. Nasirov, "Structural transformations in Cu_2Se," Neorg. Mater. **8** (6), 1144 (1970).

53. Yu. G. Asadov, K. M. Dzhafarov, and S. Yu. Asadov, "X-ray study of cation replacement in Cu_2Se," Neorg. Mater. **36** (5), 542 (2000).

54. Yu. I. Aliyev, Yu. G. Asadov, A. G. Babayev, K. M. Jafarov, F. G. Magerramova, and R. D. Aliyeva, "The polymorphous transformations in $Cu_{1.50}Zn_{0.30}Te$ and $Cu_{1.75}Cd_{0.05}Te$ crystals," Azerb. J. Phys. **18** (1), 37–43 (2012).

55. Yu. G. Asadov and G. A. Jabrailova, "Investigation of polymorphic transformations in Ag_2Se," Phys. Stat. Sol. (a) **12** K13 (1972).

56. Yu. I. Aliyev, A. G. Babayev, D. I. Ismaylov, and Yu. G. Asadov, "The structural and thermodynamic aspects of polymorphic transformations in Ag_2Se," Azerb. J. Phys. **13** (3), 56–61 (2006).

57. R. B. Baikulov and Yu. G. Asadov, "High-temperature X-ray diffraction study of the $\alpha \rightleftharpoons \beta$ transformation in CuAgSe," Neorg. Mater. **41** (4), 338–342 (2005).

58. Yu. G. Asadov, R. B. Baykulov, C. C. Hamidova, and Yu. I. Aliyev, "Polymorphic transformations in $Cu_{1\pm x}Ag_{1\pm x}Se$ ($x = 0.0, 0.4, 0.5$)," Azerb. J. Phys. **11** (4), 253 (2005).

59. Sh. K. Kyazymov, K. M. Dzhafarov, and Yu. G. Asadov, "Polymorphic transformations in $Ag_{1.5}Cu_{0.5}Se$," Neorg. Mater. **27** (2), 253 (1991).

60. Yu. G. Asadov, R. B. Baykulov, and Yu. I. Aliyev, "Phase transitions in $CuAgS_{0.5}Se_{0.5}$," Azerb. J. Phys. **11** (1–2), 62 (2005).

Translated by G. Dedkov